

**REPROGRAMMING OF ENERGY METABOLISM  
BY ONCOGENIC MAREK'S DISEASE VIRUS (MDV)  
IN CHICKEN EMBRYO FIBROBLASTS (CEFS)**

by

Nicholas Siano

A thesis submitted to the Faculty of the University of Delaware in partial fulfillment of the requirements for the degree of Master of Science in Animal Science

Summer 2014

© 2014 Nicholas Siano  
All Rights Reserved

UMI Number: 1567828

All rights reserved

INFORMATION TO ALL USERS

The quality of this reproduction is dependent upon the quality of the copy submitted.

In the unlikely event that the author did not send a complete manuscript and there are missing pages, these will be noted. Also, if material had to be removed, a note will indicate the deletion.



UMI 1567828

Published by ProQuest LLC (2014). Copyright in the Dissertation held by the Author.

Microform Edition © ProQuest LLC.

All rights reserved. This work is protected against unauthorized copying under Title 17, United States Code



ProQuest LLC.  
789 East Eisenhower Parkway  
P.O. Box 1346  
Ann Arbor, MI 48106 - 1346

**REPROGRAMMING OF ENERGY METABOLISM  
BY ONCOGENIC MAREK'S DISEASE VIRUS (MDV)  
IN CHICKEN EMBRYO FIBROBLASTS (CEFS)**

by

Nicholas Siano

Approved: \_\_\_\_\_  
Mark S. Parcels, Ph.D.  
Professor in charge of thesis on behalf of the Advisory Committee

Approved: \_\_\_\_\_  
Jack Gelb, Jr., Ph.D.  
Chair of the Department of Animal and Food Sciences

Approved: \_\_\_\_\_  
Mark Rieger, Ph.D.  
Dean of the College of Agriculture and Natural Resources

Approved: \_\_\_\_\_  
James G. Richards, Ph.D.  
Vice Provost for Graduate and Professional Education

## **ACKNOWLEDGMENTS**

I would like to thank my committee members for all their help and support through my degree. Primarily, I would like to thank Dr. Mark Parcels for his advisement and for always pushing me to be a better researcher. I would also like to thank Dr. Carl Schmidt and Dr. Maciek Antoniewicz for being on my committee and supporting my thesis along the way. Thank you to Dr. Serguei Golovan for getting my project off of the ground.

I want to thank my colleagues in the Parcels lab group for their continued support over the past year. Sabari, Upendra, Juliana, Wachen, and Yue, thank you for always being there, I will never forget the countless chicken trials. Thank you Phaedra, your help in the lab was invaluable.

Finally, I would like to thank all of my friends and family. Your continued emotional support and encouragement helped me keep my head up and make it through to reach my goal. Through good times and bad, you always had my back, I thank you!

## TABLE OF CONTENTS

LIST OF TABLES .....	vii
LIST OF FIGURES .....	viii
ABSTRACT .....	x

### Chapter

1	LITERATURE REVIEW .....	1
1.1	Marek's Disease (MD) .....	1
1.2	Marek's Disease Virus (MDV) .....	1
1.3	The Three Serotypes of MDV .....	2
1.4	MDV Genomic Organization .....	2
1.5	Pathogenesis of MDV .....	6
1.6	Control of Marek's Disease .....	7
1.7	Evolution of the Virulence of MDV-1 Field Strains .....	8
1.8	The Meq Oncogene .....	9
1.9	Meq and pp38-deletion Viruses (rMd5 $\Delta$ meq and rMd5 $\Delta$ pp38) .....	10
1.10	The Warburg Effect .....	14
1.11	Regulation of Glycolysis, the TCA Cycle, Oxidative Phosphorylation, and Glutaminolysis .....	15
1.12	Key Gene Products in the Regulation of Cellular Metabolism .....	16
1.12.1	HIF-1 $\alpha$ .....	19
1.12.2	SLC2A1 .....	19
1.12.3	HK2 .....	20
1.12.4	GAPDH .....	20
1.12.5	LDHA .....	20
1.12.6	SLC16A3 .....	21
1.12.7	PDK1 .....	21
1.12.8	GLS .....	22
1.12.9	SLC7A5 .....	22
1.12.10	SLC1A4 .....	23
1.13	Hypothesis of Research .....	23
2	MATERIALS AND METHODS .....	27

2.1	Targeted Expression Analysis: qRT-PCR.....	27
2.1.1	Cells and Viruses.....	27
2.1.2	<i>In Vivo</i> Infection and Tumor Samples.....	28
2.1.3	Sample Preparation.....	28
2.1.4	PCR Quantification.....	29
2.1.5	Primer Design.....	29
2.1.6	Statistical Analysis.....	31
2.2	Targeted Proteomic Analysis: Western Blot Analysis.....	31
2.2.1	Protein Purification.....	31
2.2.2	Antibodies.....	32
2.2.3	Western Blotting.....	34
2.2.4	Densitometric Analysis of Western Blots.....	35
3	RESULTS.....	36
3.1	Targeted Expression Analysis: qRT-PCR.....	36
3.1.1	Glycolytic Gene Expression of Oncogenic Strains.....	36
3.1.2	Glycolytic Gene Expression of Vaccine Strains and Recombinant MDVs.....	37
3.1.3	Glycolysis Gene Expression of Uninfected, MDV-infected, and MDV-transformed Spleen Cells.....	44
3.1.4	Glutaminolysis Gene Expression of Uninfected, MDV- infected, and MDV-transformed Spleen Cells.....	49
3.2	Targeted Proteomic Analysis: Western Blot Analysis.....	53
3.2.1	Glycolytic Protein Expression During Infection with MDV.....	53
3.2.2	Glutaminolytic Protein Expression During Cell Culture MDV Infection.....	54
3.2.3	Direct Comparison of Transcriptional and Translational Profiles.....	55
4	DISCUSSION.....	59
4.1	Glycolytic Gene Expression of Uninfected, MDV-infected and MDV- transformed Spleen Cells.....	59
4.2	Glutaminolytic Gene Expression of Uninfected, MDV-infected and MDV-transformed Spleen Cells.....	64
4.3	Discrepancy Between Transcript and Protein Expression Values.....	67

5	CONCLUSIONS AND FUTURE DIRECTION .....	69
5.1	Conclusions .....	69
5.2	Future Direction for this Research .....	70
	REFERENCES .....	71
Appendix		
A	WESTERN BLOT ANALYSIS RESULTS.....	84
B	PERMISSION LETTER .....	87

## LIST OF TABLES

Table 1.1:	Detailed comparison of MDV strains.....	5
Table 1.2:	Increase in number of virulent MDV strains over time.....	13
Table 1.3:	Selected gene symbols and full names .....	18
Table 1.4	Effect of multiple herpesviruses on glycolytic and glutaminolytic gene expression .....	25
Table 2.1:	List of primers used for qRT-PCR analysis. ....	30
Table 2.2	Antibodies used in the western blot analysis.....	33

## LIST OF FIGURES

Figure 1.1: Genomic orientation .....	5
Figure 1.2: Cellular events regulating the metabolism of glucose and glutamine in the average cell .....	17
Figure 3.1: Relative expression of HIF-1 $\alpha$ during cell culture MDV infection .....	38
Figure 3.2: Relative expression of SLC2A1 during cell culture MDV infection .....	39
Figure 3.3: Relative expression of HK2 during cell culture MDV infection.....	40
Figure 3.4: Relative expression of PDK1 during cell culture MDV infection .....	41
Figure 3.5: Relative expression of LDHA during cell culture MDV infection .....	42
Figure 3.6: Relative expression of SLC16A3 during cell culture MDV infection ....	43
Figure 3.7: qRT-PCR analysis of HIF-1 $\alpha$ during <i>in vivo</i> MDV infection .....	45
Figure 3.8: qRT-PCR analysis of SLC2A1 during <i>in vivo</i> MDV infection.....	45
Figure 3.9: qRT-PCR analysis of LDHA during <i>in vivo</i> MDV infection .....	46
Figure 3.10: qRT-PCR analysis of SLC16A3 during <i>in vivo</i> MDV infection.....	46
Figure 3.11: qRT-PCR analysis of SLC7A5 during <i>in vivo</i> MDV infection.....	47
Figure 3.12: qRT-PCR analysis of GLS during <i>in vivo</i> MDV infection. ....	47
Figure 3.13 qRT-PCR analysis of GAPDH during <i>in vivo</i> MDV infection .....	48
Figure 3.14: Relative expression of SLC1A4 during cell culture MDV infection .....	50
Figure 3.15: Relative expression of SLC7A5 during cell culture MDV infection .....	51
Figure 3.16: Relative expression of GLS during cell culture MDV infection.....	52
Figure 3.17 Heat summary of transcriptional expression during MDV infection .....	56
Figure 3.18 Heat summary of protein expression during MDV infection.....	57

Figure 3.19	Heat Summary of transcriptional and protein expression during TKING cell culture and transcriptional expression during TKING <i>in vivo</i> infection .....	58
Figure A1	Western blot analysis (CU-2, RB-1B, and TKING) .....	84
Figure A2	Western blot analysis (HVT, SB-1, and CVI-988) .....	85
Figure A3	Western blot analysis (Md5, Md5 $\Delta$ meq, and Md5 $\Delta$ pp38) .....	86

## ABSTRACT

Marek's disease (MD), the most prevalent clinically-diagnosed cancer in the animal kingdom, is a herpesvirus infection that rapidly induces aggressive T-cell lymphomas in chickens. This disease, caused by Marek's disease virus (MDV), a double-stranded DNA alphaherpesvirus, is prevalent worldwide. While this oncogenic herpesvirus and its cell-associated, non-sterilizing vaccinations remain good models for herpesvirus oncology and immunotherapy, respectively, the complete mechanisms of lymphoma development and progression remain unclear. The elucidation of these mechanisms remains an important topic of research.

Tumorigenesis is a multistep process in which transformed cells tend to acquire a number of biological "hallmarks of cancer" including: sustained proliferation, loss of tumor suppression, resistance to apoptosis, immortalization, angiogenesis, invasion, and metastasis. After accumulating these hallmarks of cancer, oncogenically-transformed cells shift from being benign to being fully malignant. This transition requires increased energy metabolism to support cell proliferation and growth during tumorigenesis. The increased metabolic need of these cells, in part, helped the discovery of two hallmarks of cancer: reprogramming of energy metabolism and immune evasion. German physiologist Otto Warburg had documented this switch from oxidative phosphorylation to anaerobic glycolysis and fermentation in tumorigenic cells, a process termed the *Warburg effect*.

Viruses have developed multiple processes that aid in their efficient replication within cells. The processes of genomic and structural protein replication and assembly

require substantial energy demands, and therefore it is likely that many viruses affect cellular metabolism in similar ways as cellular transformation. Specifically, MDV represents an important model of the Warburg effect due to its ability to not only replicate in multiple cell types (CEF, B-cells, T-cells, etc.), but also due to its ability to transform CD4<sup>+</sup> T-cells. This work was aimed at identifying the MDV-mediated effects on cellular metabolism during infection. In this study, we hypothesized that oncogenic MDVs induce metabolic changes during replication similar to previously documented cancers, contributing to tumorigenesis in affected birds.

To test this hypothesis, we performed qRT-PCR and Western blot analyses of MDV-infected chicken embryo fibroblasts (CEF) to determine if infection with MDV reprograms glucose and glutamine metabolism during lytic replication in cell culture. To address whether this reprogramming is MDV common, specific to oncogenic strains, or to specific gene products of MDV-1, we examined targeted gene expression during infections of CEF with: vaccine strains HVT, SB-1, and CVI-988, pathogenic MDV-1 strains: CU-2, RB-1B, rMd5, and TK (TKING), as well as two rMd5-based recombinant strains: rMd5 $\Delta$ Meq and rMd5 $\Delta$ pp38.

We found significant up-regulation in the transcription of glycolytic genes (*HIF-1 $\alpha$* , *SLC2A1*, *HK2*, *LDHA*, and *SLC16A3*) and glutaminolysis genes (*SLC7A5* and *GLS*) in cells infected with CU-2, RB-1B, rMd5 and TKING strains. Both TKING-infected CEF and TKING-transformed spleen tumors also showed biologically-significant up-regulation of *HIF-1 $\alpha$* , *SLC16A3*, and *SLC7A5* genes. Furthermore, oncogenic MDV infection of CEFs showed statistically significant increases in expression of several glycolytic and glutaminolytic genes when compared to both vaccine and rMd5-based recombinant strains. These changes in expression

were not observed by Western blot analysis, however. This discrepancy in RNA and protein levels may have been due to decreased solubility of many of the membrane-associated transport proteins. At the transcript but not the protein levels, these data support the hypothesis that virulent MDV-1 strains may affect glycolysis and glutaminolysis during lytic infection and in TKING-induced tumors. These data await further characterization via definitive assays for metabolic activity and additional assessments of protein expression (immunofluorescence or mass spectrometry).

## **Chapter 1**

### **LITERATURE REVIEW**

#### **1.1 Marek's Disease (MD)**

Some of the largest losses to the poultry industry are incurred due to Marek's disease (MD) (10). Marek's disease (MD), first described as a paralysis in laying hens by Josef Marek in 1907, was subsequently identified in flocks worldwide. Unless chickens are raised in isolated, essentially pathogen-free conditions, all flocks are considered to harbor the causative agent, Marek's disease virus, MDV (35, 71, 80). MD can affect both the nervous and visceral systems and can therefore result in general paralysis, permanent immunosuppression, and the development of T-cell lymphomas (83). Even if no symptoms are present, a flock harboring MDV can exhibit a subclinical infection that can cause decreased egg production and growth performance, leading to profit loss in table egg and meat bird industries, respectively (35). Clinical signs of MD have become increasingly severe since the early 1960s, requiring continuous use of vaccines (80). Vaccination is highly successful in preventing the progression of MD, but these vaccines do not elicit sterilizing immunity, and hence field strains of MDV remain a constant threat to poultry production, worldwide (118).

#### **1.2 Marek's Disease Virus (MDV)**

Marek's disease virus (MDV), the etiological agent of Marek's disease (MD), is a double stranded DNA virus that was originally classified as a gammaherpesvirus

due to its biological similarity with Epstein-Barr virus (EBV) (60, 80). Following electron microscopy and molecular biological studies, MDV was reclassified as an alphaherpesvirus due to its genetic similarity with herpes simplex virus (HSV) and varicella-zoster virus (VZV) (80). This cell-associated virus is able to efficiently spread among flocks, causing significant MD outbreaks (35). The use of cell-associated, non-sterilizing vaccines has proven useful in stopping MD but not MDV infection and spread (118). The use of these non-sterilizing vaccines has been associated with the evolution of MDV virulence in field strains (83, 117, 118). Therefore, the study of MDV and its vaccines remains an important, ongoing field.

### **1.3 The Three Serotypes of MDV**

Initially, MDV was described as several three agents that could be distinguished serologically (or serotypes), that is distinct agents that shared some common antigens, but could be distinguished by others. Serotype one (MDV-1), is comprised of oncogenic MDV strains and their attenuated derivatives. Pathogenic MDV-1 strains can be further classified according to their virulence into four different pathotypes; namely, classic or mild (m), virulent (v), very virulent (vv), and very virulent plus (vv+) (57, 120). Serotype 2 of MDV consists of non-oncogenic strains of MDV (18). Finally, serotype 3 is comprised of the non-pathogenic herpesvirus of turkeys (HVT) (78). The genetic basis of serotype classification is now known, and is discussed in greater detail, below.

### **1.4 MDV Genomic Organization**

Marek's disease virus (MDV) was first classified as a member of the *Gammaherpesvirinae* family, like Epstein-Barr virus (EBV). Much like this human

pathogen, MDV's ability to grow slowly in cell culture and cause T-cell lymphomas suggested that biologically, MDV belonged to this family (60, 80). Later, MDV was reclassified to the *Alphaherpesvirinae* family due to its genetic similarity with human herpesviruses 1 and 3 (HSV-1 and VZV respectively) (23, 40, 62, 80, 107). All of these alphaherpesviruses contain distinct repeat structures and follow the same general genomic organization (80, 107). These viruses contain inverted and terminal repeat regions (IRL/IRS and TRL/TRS) that flank unique long (UL) and unique short (US) genomic regions, respectively (3, 62, 80, 107). As shown in Figure 1.1, the linear genomic organization of both MDV and VZV are very similar (80).

Comparison of the genomic content of the three serotypes of MDV showed genomic differences despite the same overall structure. Currently, these viruses have been taxonomically-classified as a separate genus of *Alphaherpesvirinae* called *Mardivirus* (for **M**arek's **d**isease virus). Mardivirus-1 (MDV-1) contains oncogenic strains and their derivatives, Mardivirus-2 (MDV-2) describes the smaller non-oncogenic, naturally-occurring viruses, and *Meleagrid herpesvirus-1* describes the herpesvirus of turkeys (HVT).

The size differences for the three MDVs, and for a select group of MDV strains, is outlined in Table 1.1. These differences in size and ORF content confer the changes in virus-host interactions among the strains. The significant differences in the long and short repeat regions between the three serotypes hint at the non-pathogenic properties of MDV serotypes two and three (3, 101, 102). Located in these repeat regions are most of the virulence-associated genes of MDV-1: *meq*, pp14, RLORF4, vIL-8, vTR *etc.* Unlike these MDV-specific genes, the DNA replication and virion structural, enzymatic, and nonstructural genes are located in the unique long and short

regions. These herpesvirus-common genes are highly conserved across all three serotypes, and conserved between MDV and HSV (62).

**Table 1.1: Detailed comparison of MDV strains**

Strain	Serotype	ORFs	Overall Size	G+C Content	UL	US	TRL/IRL	TRS/IRS
rMd5	1	338	117,874	44%	113,563	10,847	13,065	12,264
CVI-988	1	478	178,311	44%	113,490	11,651	14,476	12,055
SB-1	2	524	165,994	54%	109,744	12,910	11,943	9,307
HPRS24	2	N/A	164,270	53%	109,932	12,109	11,818	8,628
HVT	3	397	159,160	47.5%	111,868	8,617	5,658	13,303

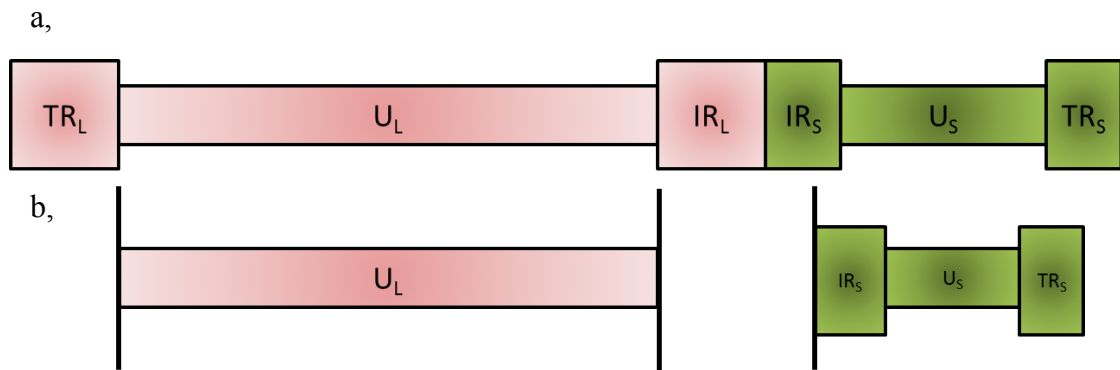


**Figure 1.1: Genomic orientation** of (a) MDV; Terminal and inverted, long and short regions ( $TR_L$ ,  $IR_L$ ,  $IR_S$ , and  $TR_S$ ) border the unique long and short regions ( $U_L$  and  $U_S$ ) of MDV; (b) VZV; The unique short ( $U_S$ ) region is again bordered by inverted and terminal short repeat regions, but the unique long ( $U_L$ ) region stands alone.

## 1.5 Pathogenesis of MDV

Marek's disease pathogenesis can be described as occurring in four phases. The exact timing and severity of these phases may vary depending on the strain used to infect the chicken and the age at which they are infected (21). Infection with MDV begins with the inhalation of feather dander shed from infected chickens. Infected dander contains free infectious virus, produced in the feather follicle epithelium (20, 80, 120). Upon reaching the lungs, these enveloped viral particles are phagocytized by lung epithelium and transferred to macrophage and B-cells. Within 24 hours, infected macrophages and B-cells travel to primary lymphoid organs where both B- and activated CD4<sup>+</sup> T-lymphocytes become infected (80).

The initial productive-restrictive phase of cytolytic infection occurs concurrently throughout the spleen, thymus, and bursa of Fabricius where the virus rapidly replicates in both B- and T-lymphocytes. In immune competent chickens (3+ weeks of age) virus lytic replication will reach its peak at 3-7 dpi and 10-14 dpi when chickens are inoculated at one day of age (19, 80, 83, 120). In the second phase of MDV infection, the infected CD4<sup>+</sup> T-cells play a critical role in latent infection and horizontal transmission. Infected T-cells can travel through the blood stream and spread infection to the feather follicle epithelium (FFE) allowing further production of free infectious virus at 10+ dpi (83).

The early cytolytic infection prompts an innate immune response (Type I and II IFNs, iNOS) which drives MDV to establish latency. This latent phase of infection can be described as the time between early cytolytic infection and cellular transformation where little to no clinical signs of disease are visible and despite the presence of the MDV genome, there exists no expression of the viral antigens (83).

Following the establishment of latency, a second wave of cytolytic infection occurs at peripheral sites, including the FFE, and typically a permanent immunosuppression of the host ensues. This immune suppression is characterized by cellular transformation and the induction of lymphomas. Cells that are transformed by MDV are indistinguishable from those seen during MDV latency, suggesting latency as a prerequisite for transformation and highlighting the importance of a wide-spread cytolytic infection and complete establishment of latency to achieve tumorigenesis (80). This lymphoproliferative phase may lead to host death as early as three weeks post infection, depending on MDV strain type, with more virulent strains causing more rapid mortality. The tumors produced during MDV infection are a “mixture of neoplastic, inflammatory, and immunologically committed and non-committed cells (19, 80, 120), however the transformed component are primarily CD4<sup>+</sup> T-cells expressing high levels of CD30, a TNFR homologous to the Reed-Sternberg antigen of Hodgkin’s lymphoma in humans (17).

## **1.6 Control of Marek’s Disease**

Shortly after the isolation and identification of MDV as the causative agent of Marek’s Disease (27), an apathogenic herpesvirus of the turkeys (HVT) was isolated that provided vaccinal protection against Marek’s disease (78). Despite its less efficient replication, the low cost and ability to provide a persistent, non-pathogenic infection made HVT a great vaccine that remains currently in use (3, 51).

Following the implementation and widespread use of HVT as the vaccine to control losses due to MDV, field strains began to appear that could break through the protection elicited by this vaccine (18, 118, 119). To combat these losses, a non-oncogenic MDV strain, SB-1, was included with HVT as a bivalent vaccine (18, 92).

This serotype 2 MDV vaccine, isolated in 1978 (93), provided increased vaccine efficacy against very virulent MDVs (18, 93).

In the early 1990's, following nearly a decade of widespread bivalent vaccine use, field strains of higher virulence evolved which overcame bivalent vaccine protection (117). To combat these losses, an attenuated MDV-1 strain from the Netherlands, CVI-988 (Rispens) was approved for use in the US (15). CVI-988 (Rispens) had been isolated in the early 1970s and through repeat serial cell-culture passage, an attenuated, highly-effective vaccine was developed (88, 89). Since 1993, several vaccine companies have produced this strain in the US commercially, and CVI-988 alone or in combination with HVT is used to vaccinate layers and broiler breeders (15, 48).

### **1.7 Evolution of the Virulence of MDV-1 Field Strains**

While MD vaccines successfully prevent tumor formation, they do not elicit sterilizing immunity and vaccinated chickens support the infection and shed of MDV-1 field strains. The survival and increased duration of MDV-1 shed from vaccinated chickens is thought to be a driver of the virulence evolution of MDV-1 field strains (118). Since its initial description in 1907, MD has evolved in disease expression (see Table 1.2) (80, 117).

When MD was first characterized by Josef Marek in 1907, he observed a low level of chronic polyneuritis in infected birds (71, 80). In the mid-1920s, the chronic polyneuritis (range paralysis) described by Marek became associated with lymphoma development, and was termed *neurolymphomatosis gallinarum* (81). Currently, MD causes a host of severe symptoms ranging from acute chronic polyneuritis, to transient paralysis, rapid lymphoma formation and acute brain edema (80).

Our laboratory, as well as others around the world, have sought the genetic basis for the evolution of MDV field strain virulence (12, 42, 99). In 2004, we reported that MDVs of different pathotype did not differ significantly in their surface glycoproteins or in the lytic infection-associated antigen pp38 (phosphoprotein 38) (99). We found that mutations in the main oncogene of MDV, Meq (for **M**arek's **E**coRI-**Q** fragment encoded protein) has shown mutations that correlate with changes in virulence.

### **1.8 The Meq Oncogene**

Meq was initially identified through the examination of mRNAs consistently expressed in MDV-induced lymphomas and derived cell lines (54). The *meq* gene encodes a 339 amino acid (aa) protein with both DNA binding and dimerization domains allowing downstream transactivation and repression activity. These Meq protein domains are similar to the Jun/Fos leucine zipper oncoproteins, both of which can associate with a multitude of other leucine zippers as well as themselves (4, 33, 69). Through multiple overexpression studies, Meq was found to increase resistance to apoptosis, induced by serum-starvation or ceramide treatment, shorten the G phase of the cell cycle, and cause morphological transformation. When Meq expression was knocked-down in an MDV-transformed cell line, the cell line decreased in proliferation (63). Deletion of Meq from the virus genome did not ablate early lytic replication of the virus, but did affect latency and the ability of MDV to cause tumors (69). These results show that Meq may not be essential for cytolytic infection, but that it is important for cellular transformation and therefore is an MDV-encoded oncogene (4, 69).

Mutations have been identified in the coding sequence of Meq that correlate with changes in MDV virulence (99). In total, four distinct domains have been identified in the *meq* gene (more than one mutation is seen in each region). Two of these have been categorized as virulence-independent, as they confer no increase or decrease in virulence with the mutations present. These mutations include a point mutation in the basic region 2 (BR2C) of the amino terminus and a cysteine to arginine substitution found in the Rb-protein binding pocket of vMDVs and vv+MDVs (LaChE -> LaRhE) (99). These mutations were found in both low and high virulence strains and therefore play no role in determining virulence.

The remaining two sets of mutations were categorized as virulence-associated. Shamblin, *et al.* found multiple low virulence strains of MDV that contain multiple direct repeats of proline flanked elements in their amino termini (99). An abundance of these repeats has been associated with transrepression, and while the numbers of repeats vary by strain, their existence in low virulence MDV suggests a functional role in pathogenicity (25, 99). Interestingly, the second virulence-associated set of *meq* mutations involves the disruption of tandem proline-rich repeats in vvMDV and vv+MDV strains. Highly virulent MDV strains have point mutations at the second position of the direct proline repeats (PPPP -> P(Q or A) PPP) (99). The proline-rich repeat regions of *meq* confer transrepression and therefore, a mutation in this site may affect this ability to repress gene expression. Furthermore, mutations in this region of *meq* could confer novel binding sites to cellular proteins (66, 99).

### **1.9 Meq and pp38-deletion Viruses (rMd5Δmeq and rMd5Δpp38)**

Aside from the oncogenes that directly cause cellular transformation and tumorigenesis, other genes thought to encode “tumor antigens” may play secondary

roles that help initiate or maintain transformation. Phosphorylated polypeptide 38 (pp38) was initially thought to be a “tumor antigen” in that has been linked with maintenance of tumors, immunosuppression, blocking of apoptosis, reactivation from latency, and lymphoid tropism (41, 84, 122). Pp38, however, was found to be associated with the reactivation of MDV from latency in tumors and cell lines, and its expression is now considered to be a hallmark of lytic infection (11, 82). Encoded at the junction of the repeats flanking the unique long region of the genome, pp38 is actually composed of two family members, pp24 and pp38, which have identical amino termini (62 aa), but divergent carboxy termini (29). Unlike *meq*, pp38 is not MDV-1 specific, although the homologs of pp38 encoded by HVT and MDV-2 are much smaller, and pp38/pp24 are expressed during the early cytolitic infection of lymphocytes *in vivo* (41, 64, 85, 122).

Interestingly, overexpression of pp38 in a transfected DF-1 cell line has shown similar metabolic changes as seen in herpes simplex virus (HSV-1) in replication in human cells (85). The increased levels of pp38 in this cell line lead to increased expression of mitochondrial succinate dehydrogenase, complex II of oxidative phosphorylation (OXPHOS) and a decreased expression of the subsequent OXPHOS complexes, resulting in an overall decreased mitochondrial adenosine-5'-triphosphate (ATP) level (64, 85). All of these changes seen in cells over-expressing pp38 are thought to be indirect effects that could perhaps contribute to cellular transformation (64, 85, 122). However, deletion of pp38 from the genome did not ablate oncogenicity, but did decrease MDV lytic infection (86).

In order to study the functions of Meq and pp38 in the context of MDV infection, recombinant deletion mutants (rMd5 $\Delta$ meq and rMd5 $\Delta$ pp38) were

constructed using an overlapping MDV cosmid strategy by Drs. Sanjay Reddy and Blanca Lupiani (69, 86). Inoculation of chickens with rMd5 $\Delta$ meq resulted in a similar level of replication to rMd5 (parent virus) at early times post-infection (cytolytic phase) but showed a marked decrease after one week (4, 69). Deletion of *meq* resulted in an attenuated virus that did not cause lymphomas, but was associated with thymic and bursal atrophy (36).

Inoculation of chickens with rMd5 $\Delta$ pp38 resulted in markedly decreased early virus replication, and increased apoptosis of infected cells (64, 69). Although tumors were still formed in rMd5 $\Delta$ pp38-infected chickens, the tumor incidence and number of tumors per chicken were greatly decreased (86).

**Table 1.2: Increase in number of virulent MDV strains over time**

<b>Years</b>	<b>Number of vMDV strains</b>	<b>Number of vvMDV strains</b>	<b>Number of vv+MDV strains</b>
1987-1989	20	80	0
1990-1992	7	71	21
1993-1995	8	58	30

### 1.10 The Warburg Effect

During transformation, cells tend to acquire a number of biological “hallmarks of cancer” including: sustained proliferation, loss of tumor suppression, increased resistance to apoptosis, immortalization, angiogenesis, invasion, and metastasis. Oncogenically-transformed cells, after accumulating these hallmarks of cancer, will progress from being benign to full malignancy. Tumorigenicity requires increased energy metabolism to support cell proliferation and growth. This increased metabolic need, in part, helped the discovery of two hallmarks of cancer: reprogramming of energy metabolism and immune evasion (47).

In a normal, healthy cell, energy metabolism occurs through glycolysis and oxidative phosphorylation producing a total of thirty-eight molecules of ATP per molecule of glucose (77, 87). Over 70 years ago, the German physiologist Otto Warburg found that there is a profound switch from oxidative phosphorylation to anaerobic glycolysis and fermentation in cancerous cells, a process termed the *Warburg effect* (114).

Viruses have evolved means to replicate efficiently within cells, including copying their genomes and assembling structural proteins, among many others (1). These processes require substantial energy demands, therefore it is likely that these viruses affect cellular metabolism in ways similar to cellular transformation by increasing cell cycle progression and increase expression of their own gene products. MDV represents a very important model in this study of the Warburg effect, as it is not only a virus that replicates within multiple types of cells (CEF, B-cells, T-cells, etc.), but has the capacity to transform them (primarily CD4+ T-cells).

### **1.11 Regulation of Glycolysis, the TCA Cycle, Oxidative Phosphorylation, and Glutaminolysis**

Cellular energy metabolism is central to all cellular activities. Most tasks carried out in a cell, whether it is the movement of proteins or the generation of macromolecules, requires large amounts of energy. This energy comes primarily in the form of ATP and is produced through the successive processes of glycolysis, the tricarboxylic acid (TCA) cycle, and oxidative phosphorylation (28).

Glycolysis is the major pathway for the oxidation of sugars that enter the cell. It most often occurs in the cytosol and can proceed without the requirement of molecular oxygen (5). Through this process, one molecule of glucose, two of adenosine diphosphate (ADP), and two of nicotinamide adenine dinucleotide ( $\text{NAD}^+$ ) are converted into two molecules each of pyruvate, ATP, and NADH (5, 34). The ATP produced through glycolysis in the cytoplasm accounts for ten percent of total cellular ATP produced in a normal cell, while the other ninety percent comes from mitochondria (34).

The mitochondria are considered the powerhouses of the cell, as successive processes of the TCA cycle and oxidative phosphorylation are localized to their outer membrane and lemmellae. The pyruvate produced through glycolysis is transported into mitochondria and converted to acetyl CoA in the matrix, where it is catabolized into  $\text{CO}_2$  (byproduct) and the electron carriers NADH and  $\text{FADH}_2$  (5). These molecules are transported deeper into the membrane where they react with oxygen in the electron transport chain to produce  $\text{H}_2\text{O}$  and generate a strong proton gradient allowing the generation of additional ATP molecules through the action of ATP synthase (5, 34, 94, 95, 110).

In addition to glucose, the non-essential amino acid glutamine has been shown to play an integral role in tumor energy metabolism (6, 116, 130). Glucose and glutamine are the only metabolites catabolized in appreciable quantities in mammalian cells and are therefore the source of almost all carbon, nitrogen, free energy, and reducing equivalents required in the cell (6, 110). The catabolism of glutamine occurs in two enzymatic steps: first, glutaminase (GLS) catabolizes the transition of glutamine into glutamate; second, glutamate dehydrogenase (GDH) converts glutamate into  $\alpha$ -ketoglutarate (130). This breakdown of glutamine into glutamate and  $\alpha$ -ketoglutarate provides cells with an abundance of nitrogen that can be used downstream in non-essential amino acid (NEAA) and carbon catabolite production. Given the central role of glutamine in this process, it is not surprising that glutamine was found to be necessary for highly proliferative cell lines (116). All of these metabolic processes are essential for the survival of a proliferating cell.

### **1.12 Key Gene Products in the Regulation of Cellular Metabolism**

The following sub-sections outline a host of genes, listed in table 1.3 and selected from these processes that outline these essential enzymatic processes. Figure 1.3 (below) depicts these major metabolic pathways while highlighting the selected genes examined in this study.

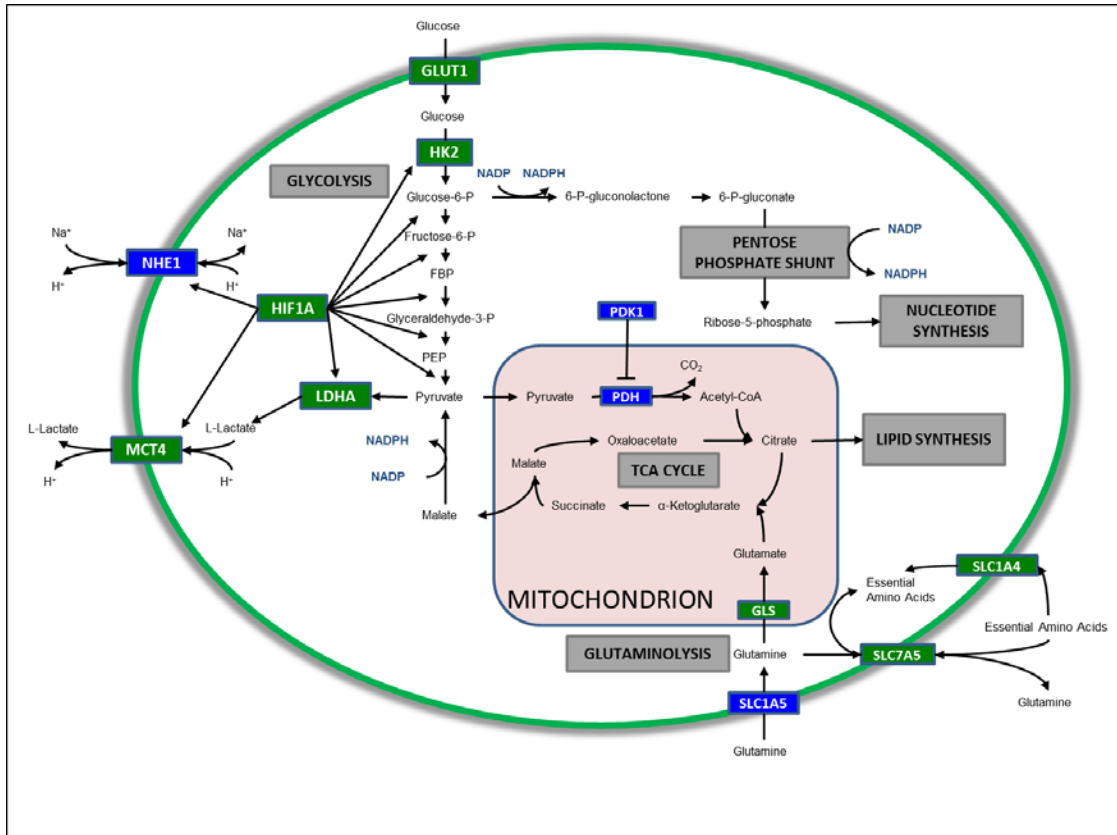


**Figure 1.2: Cellular events regulating the metabolism of glucose and glutamine in the average cell.** The diagram above shows key enzymatic steps in the regulation of glucose and glutamine catabolic processes. Genes highlighted in green were found to be significantly up-regulated in this study.

**Table 1.3: Selected gene symbols and full names**

<b>Gene Symbol</b>	<b>Gene Complete Name</b>
<b>28S RNA</b>	28S Ribosomal RNA
<b>GAPDH</b>	Glyceraldehyde 3-phosphate dehydrogenase
<b>GLS</b>	Glutaminase
<b>HIF-1<math>\alpha</math></b>	Hypoxia inducible factor 1, alpha subunit
<b>HK2</b>	Hexokinase-2
<b>LDHA</b>	Lactate dehydrogenase A
<b>PDK1</b>	Pyruvate dehydrogenase kinase, isozyme 1
<b>PIIB</b>	Peptidylprolyl isomerase B
<b>SLC16A3</b>	Solute carrier family 16, member 3
<b>SLC1A4</b>	Solute carrier family 1 (glutamate/neutral amino acid transporter) member 4
<b>SLC2A1</b>	Solute carrier family 2 (facilitated glucose transporter) member 1
<b>SLC7A5</b>	Solute carrier family 7 (amino acid transporter light chain, L system) member 5

### **1.12.1 HIF-1 $\alpha$**

Hypoxia-inducible factor (HIF) is a heterodimeric transcription factor consisting of constitutively expressed HIF-1 $\beta$  and oxygen dependent HIF-1 $\alpha$  subunits (34, 90, 94). Under normoxic conditions, the hydroxylation of two proline residues in the HIF-1 $\alpha$  subunit leads to the E3 ubiquitin ligase-mediated targeting and degradation of the HIF complex. In tissues without oxygen, such as those found in tumor microenvironments, HIF-1 $\alpha$  is not hydrolyzed and the HIF protein complex accumulates within the cell (34, 52, 53, 94). In addition to hypoxic conditions, the stabilization of HIF is possible through interaction with nitric oxide (NO), active oncogenes, and through the dysregulation of secondary metabolic processes (i.e., accumulation of succinate or fumarate) (34, 72). With its close relation to both active oncogenes and tumor microenvironments, HIF has been associated with multiple aspects of tumor growth and different viral infections including Kaposi sarcoma herpesvirus (KSHV) and Epstein-Barr virus (EBV) (94). The increased expression of this transcription factor in the context of these viral infections has been largely associated with increased glycolysis and angiogenesis, as well as decreased oxidative phosphorylation (34, 90, 95).

### **1.12.2 SLC2A1**

Solute carrier family 2, facilitated glucose transporter member 1 (SLC2A1) has been shown to be expressed in nearly all mammalian and avian tissues (44, 113). This gene, GLUT1, is responsible for the transmembrane transport of glucose, a critical first step in cellular energy metabolism. Highly conserved with 95% sequence similarity and 88% sequence identity between chicken and human protein sequences,

this glucose transporter is believed to be important for general cellular glucose transport, as opposed to other members of the SLC2 gene family (97, 113).

### **1.12.3 HK2**

Hexokinase 2 (HK2) is the second enzyme in the glycolytic pathway. Its role in phosphorylating glucose to yield Glucose-6-phosphate (G6P) is a critical, rate-limiting step in energy metabolism. Delgado *et al.*, have shown that in similar herpesvirus-associated malignancies, like Kaposi's sarcoma in humans, HK2 is up-regulated during infection to increase glucose influx into the cells (32). Furthermore, this enzyme has been shown to be up-regulated in various tumors expressing p53, a protein shown to interact with the MDV Meq protein (33, 73).

### **1.12.4 GAPDH**

Glyceraldehyde-3-phosphate dehydrogenase (GAPDH) has previously been shown to have a large array of functions including membrane fusion and transport, tDNA export, DNA repair, programmed cell death (apoptosis), and as a functional enzyme in glycolysis (106). GAPDH catalyzes the transition of glyceraldehyde-3-phosphate into D-glycerate-1,3-bisphosphate during glycolysis, effectively replenishing cellular levels of NADH during the process. Previously thought of as a housekeeping gene because of its high, ubiquitous expression in all tissues, GAPDH has recently been shown to be differentially expressed across tissues in the chicken (65).

### **1.12.5 LDHA**

The LDHA gene encodes the alpha subunit of the lactate dehydrogenase complex (LDH). This enzyme is responsible for the conversion of pyruvate and

NADH into lactate and  $\text{NAD}^+$ . It has been found that LDHA plays a role in tumorigenesis for multiple types of cancer including esophageal carcinoma and pancreatic cancer (91, 123). Knockdown of LDHA in tumor cells decreases tumor growth and increases mitochondrial respiration. Therefore this gene plays an integral role in not only tumorigenesis, but in tumor maintenance (123).

#### **1.12.6 SLC16A3**

The monocarboxylate transporter (MCT) proteins belong to solute carrier family 16. Specifically, the third member of this family (SLC16A3) is responsible for lactate and hydrogen efflux out of the cell (46). This export is critical for high lactate producing, glycolytic based cells much like the highly proliferating tumor cells (79, 110). Furthermore, these MCT proteins are found in high abundance in both white blood cells and white skeletal tissue, two cell types exhibiting increased proliferation and levels of glycolysis (79).

#### **1.12.7 PDK1**

Under normal conditions, healthy cells are able to convert one molecule of glucose, two ADP, and 2  $\text{NAD}^+$  into 2 pyruvate, 2 adenosine triphosphate (ATP), and 2 NADH through the process of glycolysis (34). This pyruvate is normally converted into acetyl-coA and then further broken down to produce more ATP. This irreversible transition into acetyl-coA is catalyzed by the pyruvate dehydrogenase complex (PDH) (34, 58, 94, 95, 97). Under decreased oxygen ( $\text{O}_2$ ) levels (hypoxia), the cells activate HIF-1 $\alpha$  as described above, which activates downstream pyruvate dehydrogenase kinase (PDK). This protein kinase is able to phosphorylate the E1 subunit of the PDH complex essentially halting its function (34, 58, 95). Halting this complex allows the

cell to shunt pyruvate away from oxidative phosphorylation to the more O<sub>2</sub> conserving lactate production for cellular energy needs (34, 94).

#### **1.12.8 GLS**

In healthy cells, and even more so in highly proliferating tumor cells, the catalysis of glutamine plays a role in both growth and cellular metabolism. This glutaminolysis process, co-induced by glutamine and leucine, can be broken down into two enzymatic steps: first, the catabolism of glutamine into glutamate by the enzyme glutaminase (GLS); second, the catabolism of glutamate into  $\alpha$ -ketoglutarate by glutamate dehydrogenase (GDH) (116). This processes not only supplies the cells with adequate ATP, but in the case of cancer cells, it allows for the continued use of the tricarboxylic acid (TCA) cycle to produce substrates needed for downstream biosynthetic pathways. The production of these substrates through the TCA cycle allows for increased cell proliferation during tumor production (103).

#### **1.12.9 SLC7A5**

Not all glutamine entering the cell is converted by glutaminase for energy production and downstream nucleotide and amino acid synthesis. Instead, some of the glutamine that enters the cell is immediately exported back out of the cell through the SLC7A5/SLC3A2 bidirectional amino acid transporter. The export of glutamine allows for the import of multiple essential amino acids (EAAs) such as leucine, an important co-inducer of glutaminolysis (116, 130). The imported EAAs can also signal general protein translation as well as be used directly for protein translation.

#### **1.12.10 SLC1A4**

In addition to the production of nucleotides and proteins, amino acids can be used for a multitude of other purposes, including pyruvate production. Proliferating tumor cells require an increased abundance of energy and use both pyruvate and glutamate production to reach their energy needs (30, 96). The glutamate and neutral amino acid transporter family, member 4 (SLC1A4/ACST1) is a major contributor of amino acid transport into cells. ASCT1 can efficiently transport alanine, serine, cysteine, and threonine into the cell (7). These amino acids, while not necessarily “essential”, are important as metabolic intermediates. Once in the cell, these amino acids are degraded to form pyruvate, which can either be shunted into the TCA cycle through acetyl-coA production, or converted into lactate and exported out of the cell (28).

#### **1.13 Hypothesis of Research**

Marek’s disease is the most costly illness to control in commercial poultry production (10). Currently, both the mechanisms of infection and tumorigenesis of Marek’s disease virus are not completely understood. Therefore, it is important to elucidate how viral infection leads to tumorigenesis so that we may provide better protection against this disease. Based on the Warburg effect and the acquisition of hallmarks of cancer that are exhibited in multiple human viral infections and tumors, we hypothesize that oncogenic Marek’s disease virus induces similar cellular metabolic changes during infection, leading to tumorigenesis in affected birds (47, 114). During infection, increased glycolysis would help produce an abundance of downstream cellular metabolites that would aid in virus particle production, as well as in sustaining the high levels of cellular proliferation seen in MDV-induced tumors. In

an increasing hypoxic environment, the large increases in both glycolysis and glutaminolysis would produce enough energy to off-set the deficit elicited by decreased oxidative phosphorylation. In addition to increased energy production in an increasingly anoxic environment, we further hypothesize that decreases in extracellular pH, due to increased lactate and hydrogen ion efflux, could negatively impact the host's immune response, allowing further replication of MDV during the lytic phase of infection, and further proliferation of latently-infected, transformed CD4+ T-cells.

A quick survey of multiple herpesvirus reveals an interesting trend in glycolytic and glutaminolytic gene expression. Table 1.4 shows changes in gene expression associated with five human herpesviruses. It is clear from the literature that there has been little documentation of metabolic changes during infection with herpes simplex virus (HSV), varicella-zoster virus (VZV), or cytomegalovirus (CMV) (22, 24, 55, 61, 74, 115, 127). On the other hand, there has been a stronger focus on metabolism for infection with both Epstein barr virus (EBV) and kaposi's sarcoma-associated herpesviru (KSHV). Infection with both gammaherpesviruses, EBV and KSHV, shows a nearly ubiquitous increase in glycolytic gene expression (31, 32, 43, 121). Furthermore, infection with EBV shows increased expression of two transporter proteins associated with glutaminolysis, SLC7A5 and SLC1A4 (128, 129). The biological similarity between these viruses and MDV and the reported increase in glycolytic gene expression gives support to our hypotheses.

**Table 1.4 Effect of multiple herpesviruses on glycolytic and glutaminolytic gene expression**

Gene Product	Herpesvirus	Effect of Virus on Product	Reference
HIF-1 $\alpha$	HSV	Increased expression	PMID:20644645(115)
	VZV	Increased expression	PMID:20644645(115)
	EBV	Increased expression	PMID:22848707(31)
	CMV	Increased expression	PMID:21481907(74)
	KSHV	Increased expression	PMID:20498071(32)
SLC2A1	CMV	Replaced by SLC2A4	PMID:21147915(127)
	EBV	Translocation to cell membrane	PMID:22848707(31)
	KSHV	Translocation to cell membrane	PMID:24422998(43)
HK2	EBV	Increased expression	PMID:24662831(121)
	KSHV	Increased expression	PMID:20498071(32)
GAPDH	HSV	Decreased expression over time	PMID:9820153(61)
LDHA	EBV	Increased expression	PMID:22848707(31)
	KSHV	Increased expression	PMID:20498071(32)
SLC16A3	EBV	Increased expression	PMID:22848707(31)
PDK1	HSV	Essential for latency	PMID:20951966(22)
	EBV	Increased expression	PMID:22848707(31)
GLS	CMV	Increased expression	PMID:19939921(24)
SLC7A5	VZV	Decreased expression	PMID:12502844(55)
	EBV	Increased expression	PMID:16446431(129)
SLC1A4	EBV	Increased expression	PMID:16474161(128)

Abbreviations: HSV: Herpes simplex virus; VZV: Varicella zoster virus; EBV: Epstein-barr virus; CMV: Cytomegalovirus; KSHV: Kaposi's sarcoma-associated herpesvirus; HIF-1 $\alpha$ : Hypoxia inducible factor 1 – alpha subunit; SLC2A1: Solute carrier family 2, member 1; HK2: Hexokinase 2; GAPDH: Glyceraldehyde-3-phosphate dehydrogenase; LDHA: Lactate dehydrogenase; SLC16A3: Solute carrier family 16, member 3; PDK1: Pyruvate dehydrogenase kinase; GLS: Glutaminase; SLC7A5: Solute carrier family 7, member 5; SLC1A4: Solute carrier family 1, member 4

For this study, we performed qRT-PCR and Western blot analyses of MDV infection of chicken embryo fibroblasts to determine if MDV strains reprogram glucose metabolism during lytic replication in cell culture. To address whether this reprogramming is MDV common or specific to oncogenic strains or to specific gene products of MDV-1, we examined the targeted gene expression during infections of CEF with: vaccine strains HVT and SB-1, MDV-1 strains: CVI-988, CU-2, RB-1B, rMd5, and TK (TKING), and recombinant strains: rMd5 $\Delta$ Meq and rMd5 $\Delta$ pp38.

## Chapter 2

### MATERIALS AND METHODS

#### 2.1 Targeted Expression Analysis: qRT-PCR

##### 2.1.1 Cells and Viruses

For all MDV propagation, secondary chicken embryo fibroblasts were prepared from 10-day-old chicken embryos obtained from specific pathogen free (SPF) flocks (Sunrise Farms, inc. Catskill, NY). All CEF cultures were grown in M199 complete medium containing 4mM L-glutamine, 1X PSN antibiotics, 1X fungizone, (Life Technologies), and 3% filtered calf serum (Life Technologies) at a constant 37°C with 5% CO<sub>2</sub>.

All MDV strains used were obtained from the stocks of the Parcels' laboratory. For MDV infections, secondary CEF were freshly plated and infected with 5000 plaque-forming units (PFU) of four oncogenic MDVs representing the different pathotypes of MDV: CU2 (an m/vMDV, obtained originally from Dr. K.A. Schat, Cornell University), RB-1B (a vvMDV, originally obtained from Dr. K.A. Schat), rMd5 (originally obtained from Dr. Sanjay Reddy, Texas A & M University), and TKING (TK, a vv+MDV, originally obtained from Dr. John K. Rosenberger, University of Delaware) and three MDV vaccine strains (HVT, SB-1, and CVI-988, all obtained from Merial, Inc., Gainesville, GA).

Another subset of secondary CEF cultures were infected with 10,000 PFU of rMd5Δmeq and rMd5Δpp38 strains (originally obtained from Dr. Sanjay Reddy) (69,

86). All viral infections were performed in triplicate as biological replicates (n=3). Cells were harvested five days post-infection (dpi), placed directly into lysis buffer, stored at -80°C, and later prepared for RNA and protein purification, as detailed below.

### **2.1.2 *In Vivo* Infection and Tumor Samples**

To provide data from *in vivo* infection, spleens were collected from broilers during a vaccine efficacy trial. Broiler chickens (Hubbard X Cobb) were infected via contact with the vv+MDV (TKING) strain of MDV. Spleen tumor samples (n=3) and infected spleen samples (n=3) were collected from euthanized chickens at forty-nine days post-placement. Spleens (n=3) were also collected from non-infected, non-vaccinated chickens on the same day to serve as negative controls for infection. All collected tissues were placed in RNA Later (Ambion Inc., Austin, TX) and stored at -80°C for future RNA purification.

### **2.1.3 Sample Preparation**

Total RNA was extracted from all samples (infected CEF, spleens and tumors) using an AllPrep DNA/RNA/Protein Mini Kit (Qiagen, USA) according to the manufacturer's instructions. Sample quantity and quality (260:280nm ratio) were measured using a ThermoFisher Scientific Nanodrop 1000 Spectrophotometer (Thermo Scientific, Waltham, MA). Reverse transcription was performed on 20µl reactions using 1µg of total RNA and random hexamers from a High Capacity cDNA Reverse Transcription Kit (Applied Biosystems, USA). Reverse transcription was carried out in the following four steps: Step 1: 25°C for 10 min; Step 2: 37°C for 120 min; Step 3: 85°C for 5 min; Step 4: 4°C until samples are removed. The final cDNA

samples were diluted tenfold in nuclease-free water and stored at -80°C for later analysis.

#### **2.1.4 PCR Quantification**

Quantitative real time PCR was carried out using a mixture of 10 µl iQ™ SYBR® Green Supermix (Bio-Rad, Hercules, CA), 8.2µl of ddH<sub>2</sub>O, 1 µl of diluted cDNA sample, and 0.4 µl of forward and reverse primers in a Bio-Rad iCycler iQ5 PCR Thermal Cycler. The following cycle times were used: cDNA denaturation at 95°C for 3 minutes was followed by 40 cycles of a two-step procedure (Step 1: 95°C for 10 seconds; Step 2: 58°C for 30 seconds). Following these amplification steps, melt curves were produced using the following steps: Step 1: 95°C for 1 minute; Step 2: 55°C for 1 minute; Step 3: 81 cycles of increasing temperatures from 55°C to 95°C at 10 second, 0.5°C intervals per cycle. Melt curve analysis was performed to identify and remove any sample abnormalities.

#### **2.1.5 Primer Design**

Chicken specific sequences for all target genes were obtained through the Ensembl Genome Browser. Quantitative real-time PCR primers (Table 2.1) were designed across introns using Integrated DNA Technologies PrimerQuest (SM) online software (<http://www.idtdna.com>). All primers were selected to have an annealing temperature approximately 58°C.

**Table 2.1: List of primers used for qRT-PCR analysis.**

<b>Gene</b>	<b>Primer Sequence</b>	<b>Amplicon Size (bp)</b>	<b>Accession #</b>
<b>28S RNA</b>	GGTATGGGCCCGACGCT CCGATGCCGACGCTCAT	160	FM165415.2
<b>GAPDH</b>	GGAGTCCACTGGTGTCTTCA AGCACCACCCTTCAGATGAG	234	NM_204305
<b>GLS</b>	AATGTCATGGGCTTGATGTGCTGG ATCACCACCTTCTCTGCGAGGAT	814	NM_001031248
<b>HIF-1<math>\alpha</math></b>	AGGAACTCCTGGGTCGTTCAATCT ACCCAGACGTAGCCACCTTGTTTA	301	NM_204297.1
<b>HK2</b>	TGAAGCGGAGGATGAGGGTTGAAA ACACGTATGTGGGCAGCATCTTCA	90	NM_204212.1
<b>LDHA</b>	AAGAGTGCACCCAATCTCTACAGC CTGCCAGTACACAAGGAACACTT	268	NM_205284.1
<b>PDK1</b>	ATCCAGTGACCTCACAGAATGTGC GCTTCCAATGTGTTTAGGATGAGCTGG	385	NM_001031352.3
<b>PPIB</b>	GAGAAAGGGTTTCGGCTTCA CAGCTTGAAGTTCTCGTCAGG	311	NM_205461.1
<b>SLC16A3</b>	AGTGACACTGCATGGATTTCTCC AAAGCGATTGACGCACACGCTACA	487	NM_204663.1
<b>SLC1A4</b>	GGACTTATCACACCATTTGCCACTGC CCATCCATGTTTACAGTTGCACCA	1277	XM_001232899
<b>SLC2A1</b>	CCGCAATGAGGAGAACAAGCCAA TCTCTCTCATATTTGCCGGCTCT	197	NM_205209.1
<b>SLC7A5</b>	ATGATTCACCCGAGGCTTCTCACT TGTCATTGGAGAAGGCGTAGAGCA	436	NM_001030579

### **2.1.6 Statistical Analysis**

In order to calculate relative gene expression, the equation of Vandesompele *et al.* was used to normalize all experimental threshold cycle (Ct) values to the geometric mean of three housekeeping genes (28S RNA, PPIB, and GAPDH) and to compare these normalized values to an average mock sample value (111). Oncogenic, vaccine, and recombinant strain samples (test conditions), were compared back to an average mock sample (reference condition). A Tukey's honest significant difference test (HSD) was conducted using the JMP statistical analysis software (SAS Institute, Cary, NC) to compare expression values between oncogenic, vaccine, and recombinant infection to search for significant differences.

*In vivo* samples were also normalized to the geometric mean of three housekeeping genes (28S RNA, PPIB, and  $\beta$ -actin). Relative expression for the *in vivo* data set was obtained through the comparison of the tumor groups to both the infected groups and the uninfected control groups and the comparison of the infected group to the control group. All statistically significant data is represented at the  $P < 0.05$  level.

## **2.2 Targeted Proteomic Analysis: Western Blot Analysis**

### **2.2.1 Protein Purification**

For protein analysis, the following strains and total plaque forming units (PFU, as determined by back-titration) were plated onto triplicate 100 mm dishes of secondary CEF: CU2 (40,000 PFU), RB-1B (30,000 PFU), rMd5 (90,000 PFU), TKING (23,000 PFU); HVT (9,000 PFU), SB-1 (33,000 PFU), CVI-988 (41,000 PFU); and recombinant strains: rMd5 $\Delta$ meq (30,000 PFU) and rMd5 $\Delta$ pp38 (33.33

PFU). All cultures were either directly harvested or passaged until >60% of the cells were infected on each dish.

When cells were confluent and at peak levels of infection, medium was removed and monolayers were washed with 10 mls of cold 1X PBS, pH 7.4. Cells were harvested in 0.5 mls radioimmnoprecipitation assay (RIPA) buffer (20mM Tris, 150mM NaCl, 1% IGEPAL, 0.1% SDS, 10% glycerol, 1x aprotinin, 1x pepstatin A, 1x leupeptin, 1x PMSF, 1mM NaF, and 1mM Na-orthovanadate). Cells were collected using a cell scraper and pipetted into 1.5 ml Eppendorf tubes. Cells were lysed via three snap freeze/thaw cycles (between liquid nitrogen and a 37°C bath) followed by a 30 minute incubation step on ice with vortexing at 5 minute intervals.

Cellular debris was pelleted at 10,000 RPM for 10 minutes at 4°C and the cell lysates were aliquoted to five 1.5 ml Eppendorf tubes and stored at -80°C. All protein samples were quantified following the Pierce® BCA Protein Assay Kit (Thermo Scientific, Waltham, MA) micro protocol and dye absorbance was determined using a SpectraMax M2 plate reader (Molecular Devices, Sunny Vale, CA). Diluted BSA standards were used to generate a standard curve for protein concentration.

### **2.2.2 Antibodies**

Primary, polyclonal antibodies were selected for all target genes and ordered from Sigma Aldrich (Sigma-Aldrich, St. Louis, MO). The primary antibodies, animal source and dilutions used are given in (Table 2.2, below). Antibodies were diluted in a blocking buffer consisting of TBST (Tris-buffered saline with 0.05% Tween 20), with 3% bovine serum albumin (BSA), and 1% goat serum. Secondary antibodies were diluted to 1:500 to 1:5000, as noted, in blocking buffer.

**Table 2.2 Antibodies used in the western blot analysis**

<b>Antibody Specificity</b>	<b>Host</b>	<b>Type</b>	<b>Size (kDa)</b>	<b>Chicken Homolog Uniprot ID</b>	<b>Company</b>	<b>Dilution</b>
<b>GAPDH</b>	Mouse	Monoclonal	35.70	P00356	USBiological	1:750
<b>SLC2A1 (GLUT1)</b>	Rabbit	Polyclonal	54.09	P46896	Sigma Aldrich	1:1000
<b>HIF-1<math>\alpha</math></b>	Rabbit	Polyclonal	90.54	Q9YIB9	Sigma Aldrich	1:1000
<b>HK2</b>	Rabbit	Polyclonal	102.42	Q8AYP7	Sigma Aldrich	1:1000
<b>SLC16A3</b>	Rabbit	Polyclonal	58.18	Q90632	Sigma Aldrich	1:1000
<b>GLS</b>	Rabbit	Polyclonal	69.90	F1NSV7	Sigma Aldrich	1:1000
<b>LDHA</b>	Rabbit	Polyclonal	36.51	P00340	Sigma Aldrich	1:1000
<b>SLC1A4</b>	Rabbit	Polyclonal	56.06	E1BRV6	Sigma Aldrich	1:1000
<b>SLC7A5</b>	Rabbit	Polyclonal	56.45	F1NEI2	Sigma Aldrich	1:1000
<b>Secondary Antibody</b>					<b>Company</b>	<b>Dilution</b>
Stabilized Goat Anti-Rabbit IgG (H+L), Peroxidase Conjugated					Thermo Scientific	1:500
Stabilized Goat Anti-Mouse, Peroxidase Conjugated					Thermo Scientific	1:5000

### **2.2.3 Western Blotting**

Equivalent quantities of protein sample and 2X protein loading buffer (50 mM Tris-HCl, pH6.8, 10% Glycerol, 2% SDS, 100mM Dithiothreitol (DTT), 0.1% Bromophenol Blue (after dilution to 1X)) were mixed and boiled for 5 minutes. A total of 40 µg of each protein sample was loaded per lane into a 1.5 mm thick, 10% Tris-glycine pre-cast gel (Jule Biotechnology, Milford, CT) for electrophoresis using a Bio-Rad Mini Protean II gel apparatus (Bio-Rad, Hercules, CA). Gels were run at 100V (constant voltage), and subsequently transferred to a 0.45 µm nitrocellulose membrane (Whatman, Maidstone, UK) at 100 mAmps (constant current) for 1.5 hours. After transfer, membranes were air dried overnight to covalently link proteins to the nitrocellulose.

Membranes were initially wetted in TBST and incubated for 2 hours in blocking buffer with agitation at room temperature. Blots were probed with antibody diluted in blocking buffer for 1 hour, washed in TBST three times for 5 minutes each, and probed with diluted secondary antibody (appropriate HRP conjugate) for 30 min, with agitation at room temperature.

Following incubation in secondary antibody, blots were washed in TBST three times for 5 minutes each. After the final wash, Supersignal® West Dura Extended Duration Substrate, a light-emitting substrate, (Thermo Scientific, Waltham, MA) was prepared and added to the blot for a 5 minute incubation step. Following the application of the substrate, blots were wrapped in saran wrap, taped to a piece of Whatman filter paper, and placed in a Kodak X-omatic cassette with GeneMate Blue Lite Autoradiography Film (BioExpress, VWR, Radner, PA) for autoluminography. Exposure times were adjusted based on the level of signal from the blot. Films were

then developed in a Kodak X-OMAT 1000 autoprocessor (Kodak, Rochester, NY) for visualization.

Following film exposure and processing, blots were washed in 1X PBS (phosphate buffered saline) for 5 minutes. After this initial wash step, blots were submerged in Restore™ Western Blot Stripping Buffer (Thermo Scientific, Waltham, MA) and agitated for 15 minutes. Subsequently, blots were washed with 1X PBS for 5 minutes, exposed to Supersignal® West Dura Extended Duration Substrate, and tested to make sure antibodies were properly stripped. Upon confirmation, blots were washed for 5 minutes with 1X PBS, incubated in blocking buffer for 2 hours, and probed with a different antibody. This stripping and re-probing protocol was repeated until all primary antibodies were tested.

#### **2.2.4 Densitometric Analysis of Western Blots**

Western blot films were scanned for densitometric analysis using an HP Deskjet 4200 series scanner. Scanned images were then analyzed using Image Processing and Analysis in Java (ImageJ, NIH, Bethesda, MD) software tool. Using this software, protein band densities were acquired and normalized to GAPDH expression for each blot. Following normalization, all infected samples were compared to mock infected CEFs to determine any significant protein changes caused by with MDV infection. A Tukey's honest significant difference test (HSD) was run to compare not only individual strains to one another, but among groups of strains (oncogenic, vaccine, recombinant).

## Chapter 3

### RESULTS

#### 3.1 Targeted Expression Analysis: qRT-PCR

##### 3.1.1 Glycolytic Gene Expression of Oncogenic Strains

To assess the relative RNA levels of select glycolysis- and glutaminolysis-associated genes during MDV lytic infection of CEF, we performed quantitative real-time PCR (qRT-PCR) using the primers shown in Table 2.1. Figures 3.1 – 3.6 show the relative expression for the target glycolytic genes in cell culture. As seen in figure 3.1, using a 2-fold difference in expression as a biologically significant cutoff, the expression of transcription factor HIF-1 $\alpha$  is significantly increased during infection with all oncogenic MDV strains.

The induction of glucose into the cell by SLC2A1, thought to be in part controlled by HIF-1 $\alpha$ , was found to have significantly increased expression during infection with three of the four oncogenic strains (CU2, RB-1B, and TKING). As one of the rate-limiting steps of true glycolysis, hexokinase 2 (HK2) was found to be up-regulated only during infection with the RB-1B strain. Pyruvate dehydrogenase kinase (PDK1) failed to show any significant change during infection with oncogenic MDV. The final lactate producing step in glycolysis, catabolized by LDHA was found to be significantly up-regulated only during infection with CU2. Finally, the expression of SLC16A3, responsible for lactate and hydrogen ion (H<sup>+</sup>) export from the cell, is significantly increased during infection with all oncogenic strains tested. A

Tukey's Honest Significant Difference (HSD) confirmed a statistical difference between the different groups of MDV strains tested (oncogenic, vaccine, or recombinant) for almost all genes, as seen in figures 3.1 – 3.6.

### **3.1.2 Glycolytic Gene Expression of Vaccine Strains and Recombinant MDVs**

Infection with vaccine strains revealed no significant differences from mock infection for any of the genes tested. When infected with the recombinant strains, rMd5 $\Delta$ meq and rMd5 $\Delta$ pp38, most of the glycolytic genes were significantly downregulated. Again, the transcription factor HIF-1 $\alpha$  and the cellular glucose transporter SLC2A1 showed both statistically and biologically significant downregulation during infection with these strains. Both HK2 and the PDK1 genes showed no significant difference from mock during infection. Lactate production was downregulated during infection with rMd5 $\Delta$ pp38, but not rMd5 $\Delta$ meq. Finally, SLC16A3 expression and therefore lactate and hydrogen ion export expression were significantly decreased during infection with these recombinant strains.

As noted above, a Tukey's HSD analysis shows a statistical difference between groups of MDV strains for half of the genes observed (HIF-1 $\alpha$ , SLC2A1, and LDHA). The use of these MDV strains allows for the comparison of normal MDV viral infection and MDV viral infection without an important contributing oncogene (Meq or pp38).

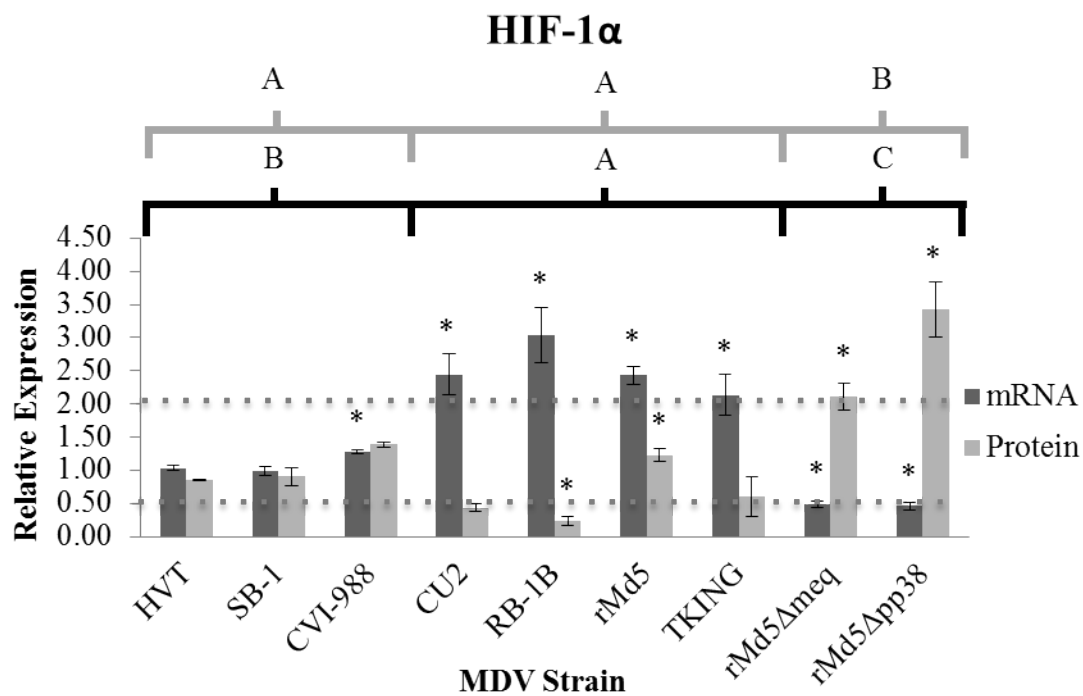


**Figure 3.1: Relative expression of HIF-1 $\alpha$  during cell culture MDV infection.** Data are expressed as mean relative expression of three samples (n=3) by strain with error bars representing the standard error. An asterisk denotes statistically significant differences from an average mock sample at the p<0.05 level, dotted lines represent a 2-fold change in expression as the biological significance, and the letters at the top represent a Tukey's HSD analysis for mRNA (black) and protein (gray) levels.

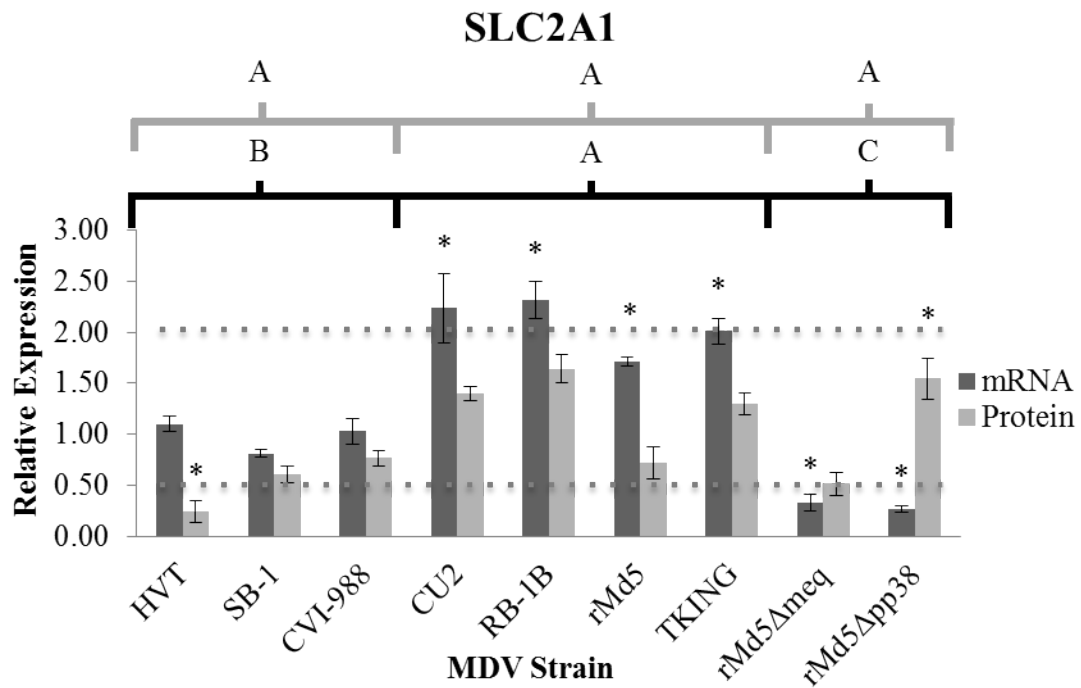


**Figure 3.2: Relative expression of SLC2A1 during cell culture MDV infection.** Data are expressed as mean relative expression of three samples (n=3) by strain with error bars representing the standard error. An asterisk denotes statistically significant differences from an average mock sample at the  $p < 0.05$  level, dotted lines represent a 2-fold change in expression as the biological significance, and the letters at the top represent a Tukey's HSD analysis for mRNA (black) and protein (gray) levels.

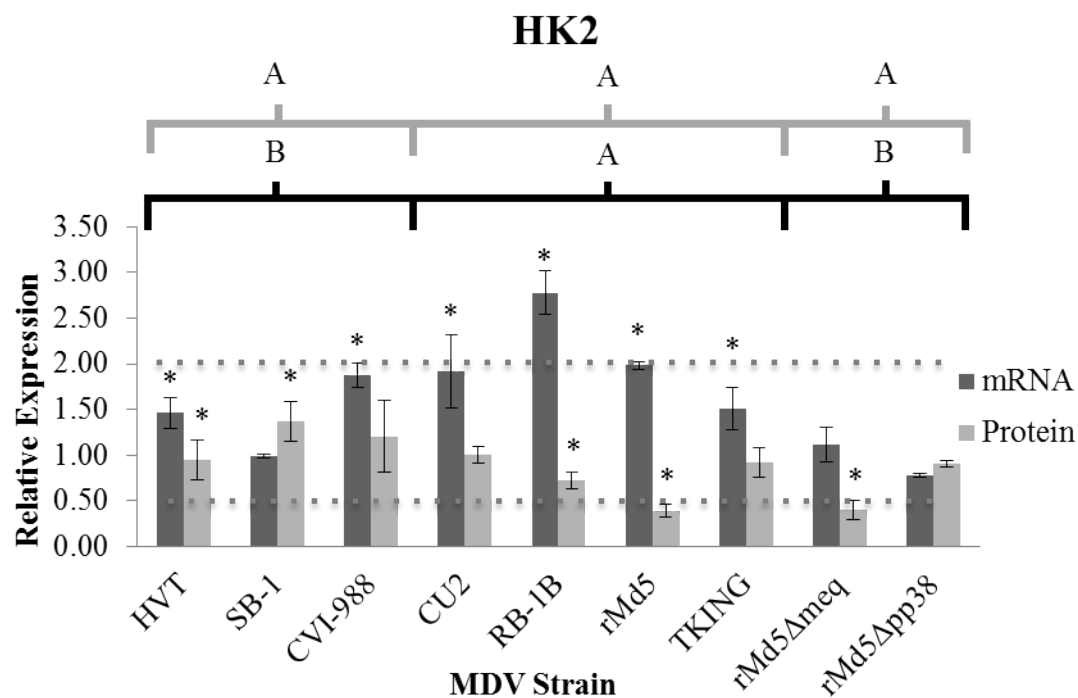


**Figure 3.3: Relative expression of HK2 during cell culture MDV infection.** Data are expressed as mean relative expression of three samples (n=3) by strain with error bars representing the standard error. An asterisk denotes statistically significant differences from an average mock sample at the  $p < 0.05$  level, dotted lines represent a 2-fold change in expression as the biological significance, and the letters at the top represent a Tukey's HSD analysis for mRNA (black) and protein (gray) levels.

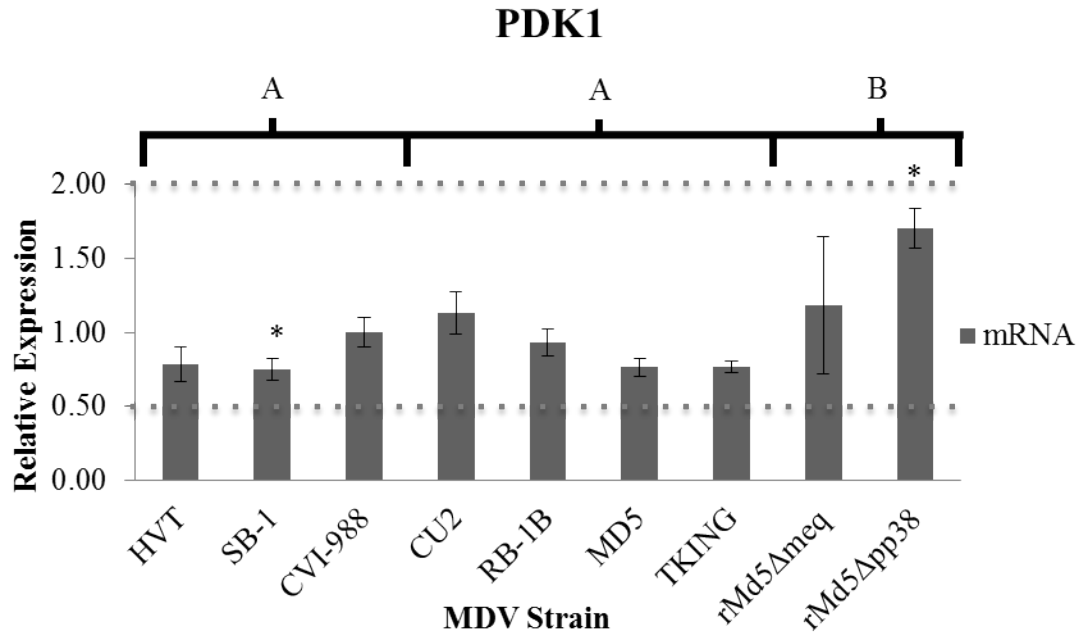


**Figure 3.4: Relative expression of PDK1 during cell culture MDV infection.** Data are expressed as mean relative expression of three samples (n=3) by strain with error bars representing the standard error. An asterisk denotes statistically significant differences from an average mock sample at the  $p < 0.05$  level, dotted lines represent a 2-fold change in expression as the biological significance, and the letters at the top represent a Tukey's HSD analysis for mRNA (black) and protein (gray) levels

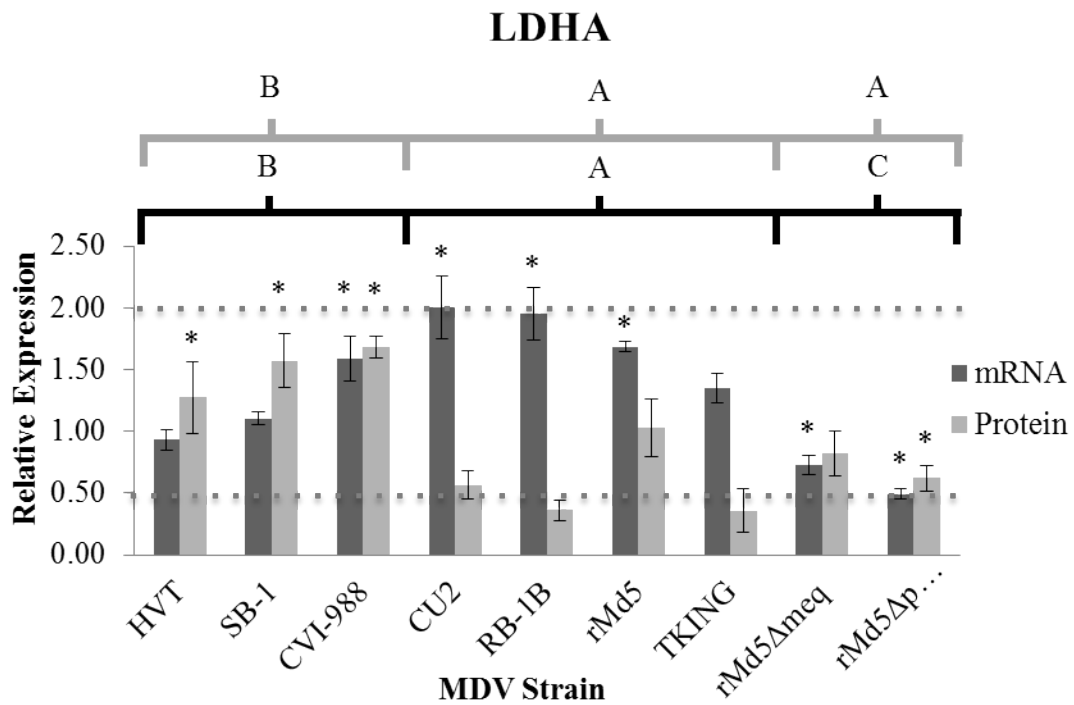


**Figure 3.5: Relative expression of LDHA during cell culture MDV infection.** Data are expressed as mean relative expression of three samples (n=3) by strain with error bars representing the standard error. An asterisk denotes statistically significant differences from an average mock sample at the  $p < 0.05$  level, dotted lines represent a 2-fold change in expression as the biological significance, and the letters at the top represent a Tukey's HSD analysis for mRNA (black) and protein (gray) levels.

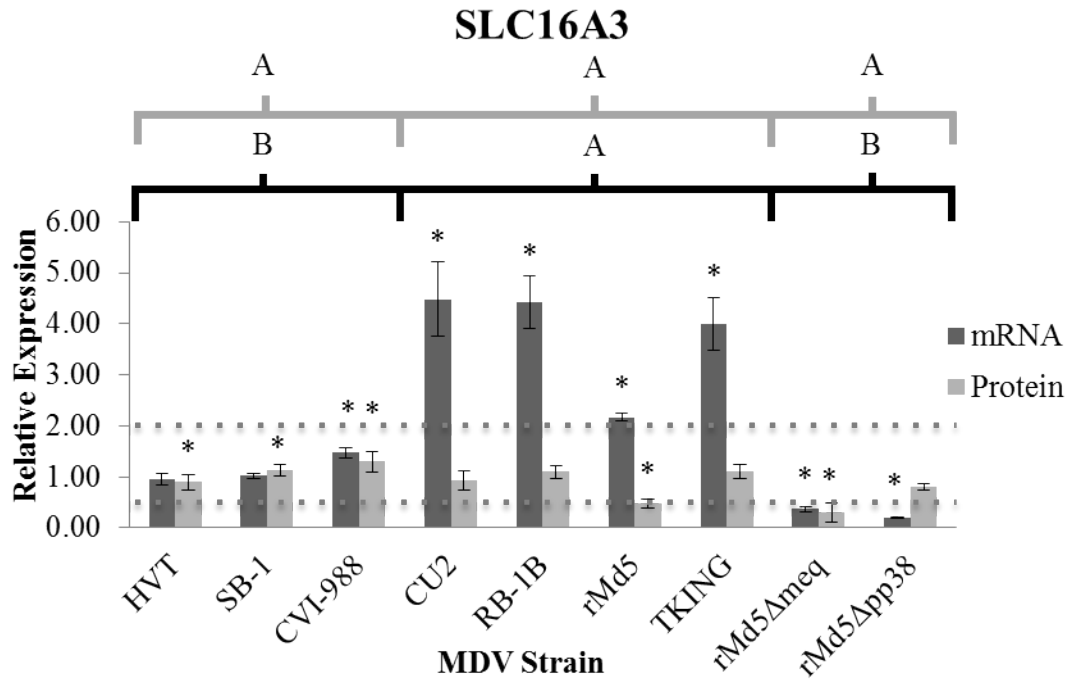


**Figure 3.6: Relative expression of SLC16A3 during cell culture MDV infection.** Data are expressed as mean relative expression of three samples (n=3) by strain with error bars representing the standard error. An asterisk denotes statistically significant differences from an average mock sample at the  $p < 0.05$  level, dotted lines represent a 2-fold change in expression as the biological significance, and the letters at the top represent a Tukey's HSD analysis for mRNA (black) and protein (gray) levels.

### **3.1.3 Glycolysis Gene Expression of Uninfected, MDV-infected, and MDV-transformed Spleen Cells**

When normalized to PPIB, 28S RNA, and  $\beta$ -actin, comparisons of spleen tumors to both uninfected spleen cells and non-tumorous, MDV-infected spleens using the  $\Delta\Delta_{Ct}$  method revealed significant up-regulation for both GAPDH and SLC16A3. As seen in Figures 3.7 and 3.8, despite large fold changes for both HIF-1 $\alpha$  and SLC2A1, this change in expression was not found to be significant between samples. A paired t-test comparing tumors and non-tumorous samples from the same spleens revealed no significant differences.

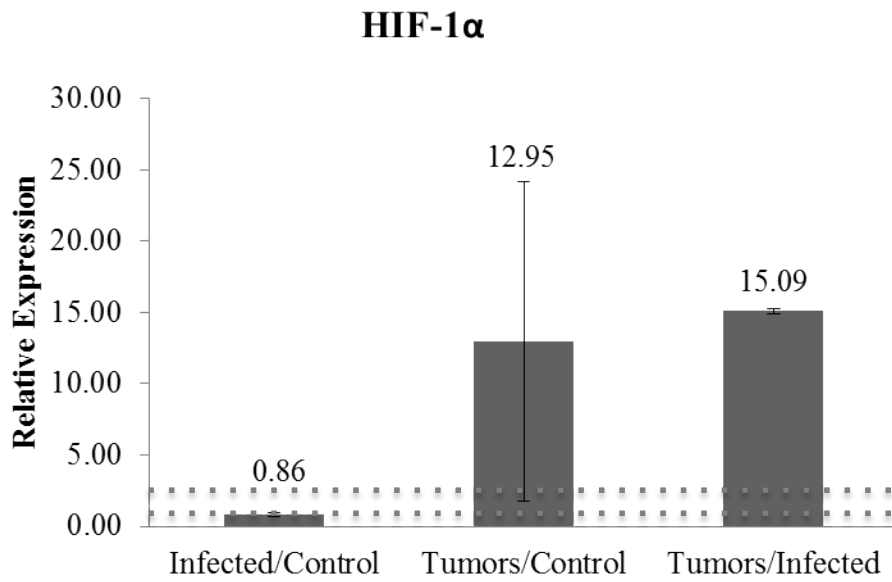


**Figure 3.7: qRT-PCR analysis of HIF-1 $\alpha$  during *in vivo* MDV infection.** Tumor and non-tumorous, infected samples were compared to splenic samples from non-vaccinated, non-infected chickens.

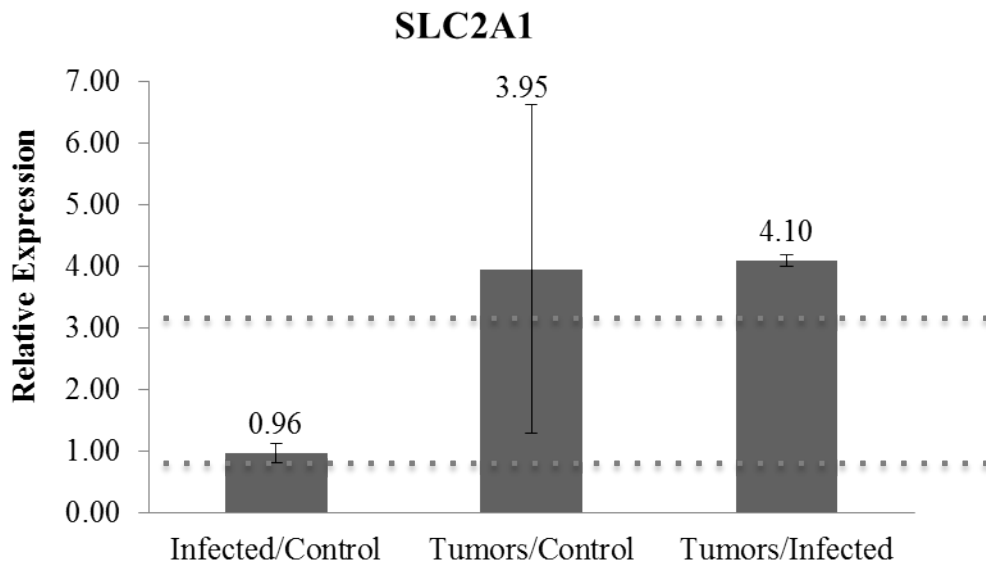


**Figure 3.8: qRT-PCR analysis of SLC2A1 during *in vivo* MDV infection.** Tumor and non-tumorous, infected samples were compared to splenic samples from non-vaccinated, non-infected chickens.

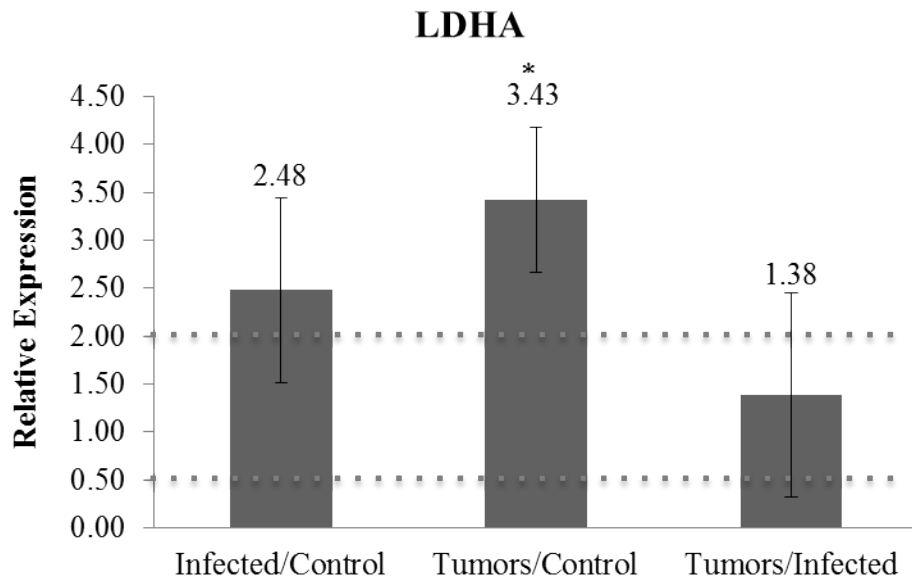


**Figure 3.9: qRT-PCR analysis of LDHA during *in vivo* MDV infection.** Tumor and non-tumorous, infected samples were compared to splenic samples from non-vaccinated, non-infected chickens.

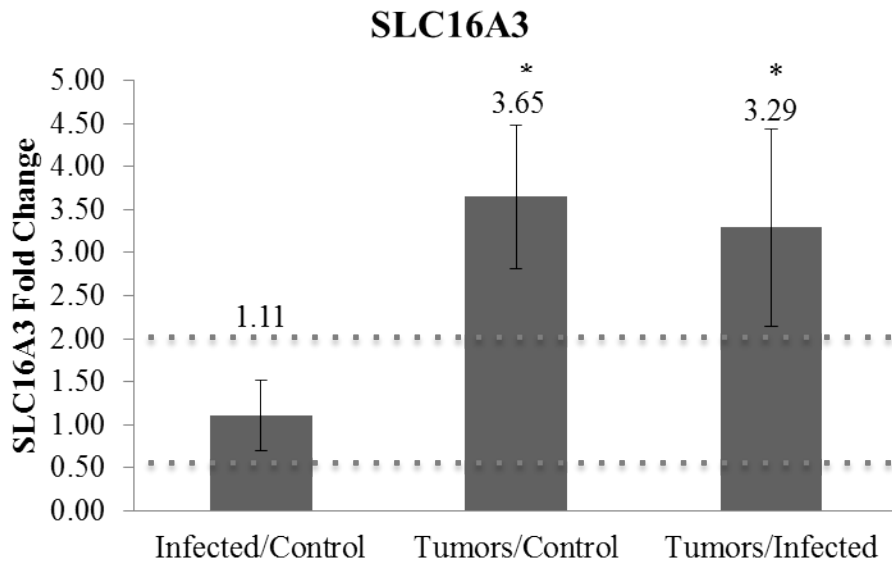


**Figure 3.10: qRT-PCR analysis of SLC16A3 during *in vivo* MDV infection.** Tumor and non-tumorous, infected samples were compared to splenic samples from non-vaccinated, non-infected chickens.

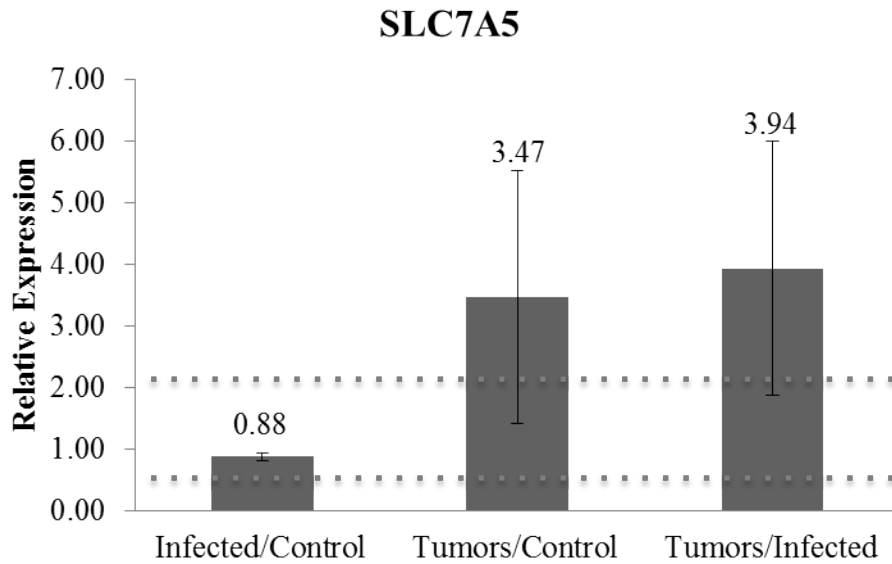


**Figure 3.11: qRT-PCR analysis of SLC7A5 during *in vivo* MDV infection.** Tumor and non-tumorous, infected samples were compared to splenic samples from non-vaccinated, non-infected chickens.

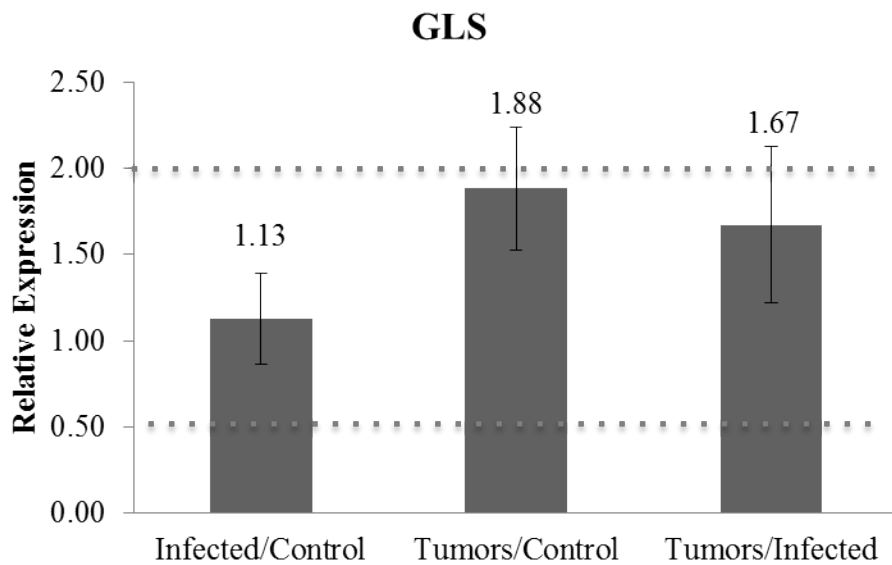


**Figure 3.12: qRT-PCR analysis of GLS during *in vivo* MDV infection.** Tumor and non-tumorous, infected samples were compared to splenic samples from non-vaccinated, non-infected chickens.

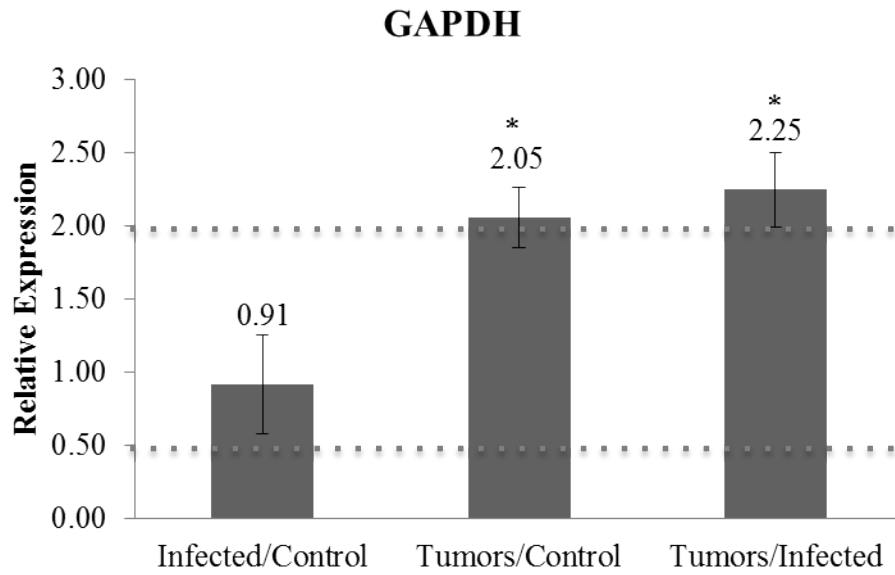


**Figure 3.13** qRT-PCR analysis of GAPDH during *in vivo* MDV infection. Tumor and non-tumorous, infected samples were compared to splenic samples from non-vaccinated, non-infected chickens.

### **3.1.4 Glutaminolysis Gene Expression of Uninfected, MDV-infected, and MDV-transformed Spleen Cells**

Our results show little biologically significant changes in glutaminolytic gene expression during infection with oncogenic MDV (i.e., greater than 2 fold changes in expression). Figures 3.14 and 3.15, below, show that while the transport of amino acids into the cell through SLC1A4 expressed no significant change during oncogenic infection, the co-transport of essential amino acids and glutamine into and out of the cell respectively by SLC7A5 was up-regulated during infection with both CU2 and TKING strains. In addition, one of the major enzymatic steps of glutaminolysis, catabolized through the activity of glutaminase (GLS) showed significantly increased expression during infection with both RB-1B and Md5 MDV strains, shown in figure 3.16.

During infection with vaccine MDV strains, figure 3.15 shows that infection with HVT is the only condition in which SLC7A5 expression was significantly decreased. In all other cases, there was no significant difference from mock infection. As seen in figure 3.14, infection with rMd5 $\Delta$ pp38 caused decreased SLC1A4 expression. The glutamine transporter SLC7A5 has significantly lower expression during infection with both recombinant strains (rMd5 $\Delta$ meq and rMd5 $\Delta$ pp38). Finally, there were no significant changes in glutaminase expression during infection with these strains. A Tukey's HSD analysis shows statistically significant similarity between vaccine and recombinant strain infection for both transporter genes. The tumor samples tested showed numerical increases in the SLC7A5 transporter, but they were not statistical significant.

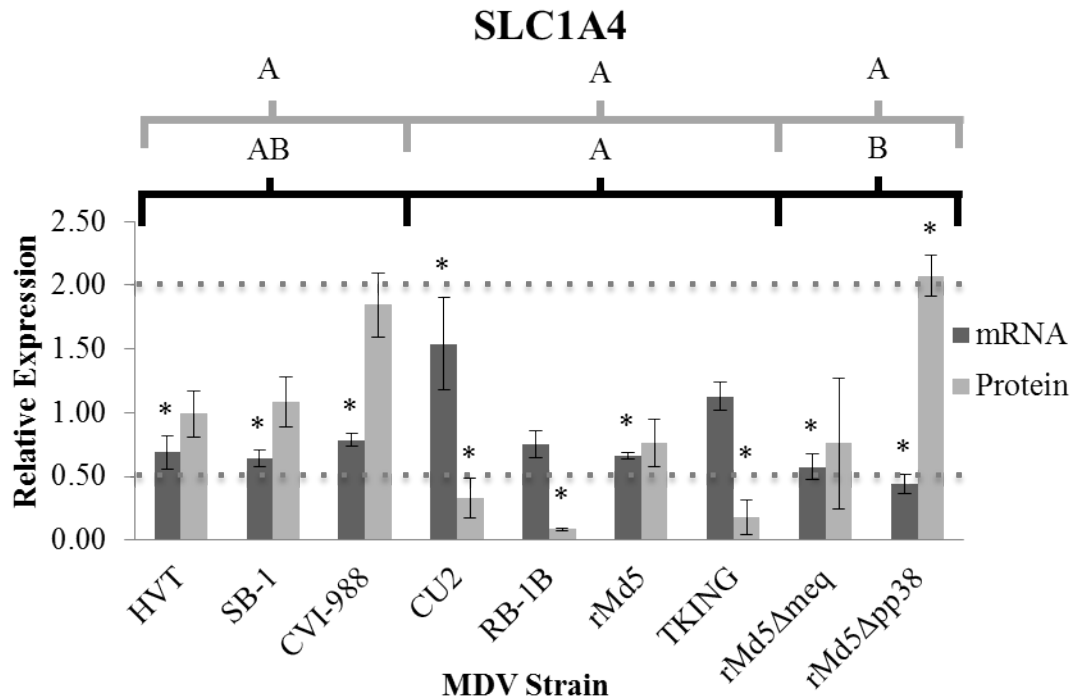


**Figure 3.14: Relative expression of SLC1A4 during cell culture MDV infection.** Data are expressed as mean relative expression of three samples (n=3) by strain with error bars representing the standard error. An asterisk denotes statistically significant differences from an average mock sample at the  $p < 0.05$  level, dotted lines represent a 2-fold change in expression as the biological significance, and the letters at the top represent a Tukey's HSD analysis for mRNA (black) and protein (gray) levels.

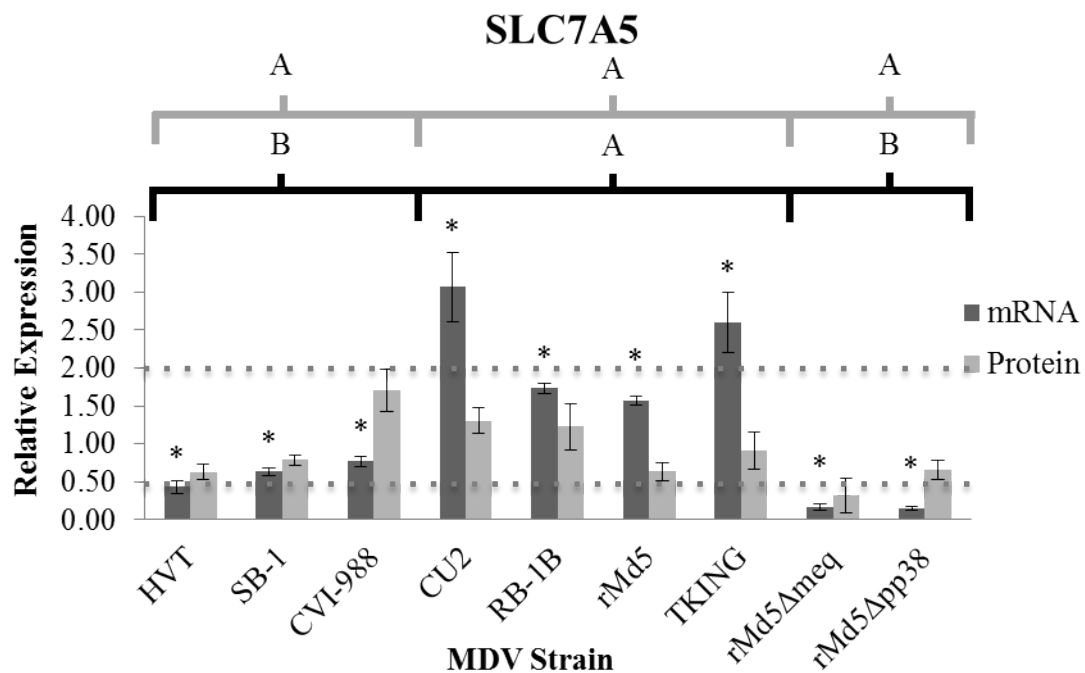


**Figure 3.15: Relative expression of SLC7A5 during cell culture MDV infection.**

Data are expressed as mean relative expression of three samples (n=3) by strain with error bars representing the standard error. An asterisk denotes statistically significant differences from an average mock sample at the  $p < 0.05$  level, dotted lines represent a 2-fold change in expression as the biological significance, and the letters at the top represent a Tukey's HSD analysis for mRNA (black) and protein (gray) levels.

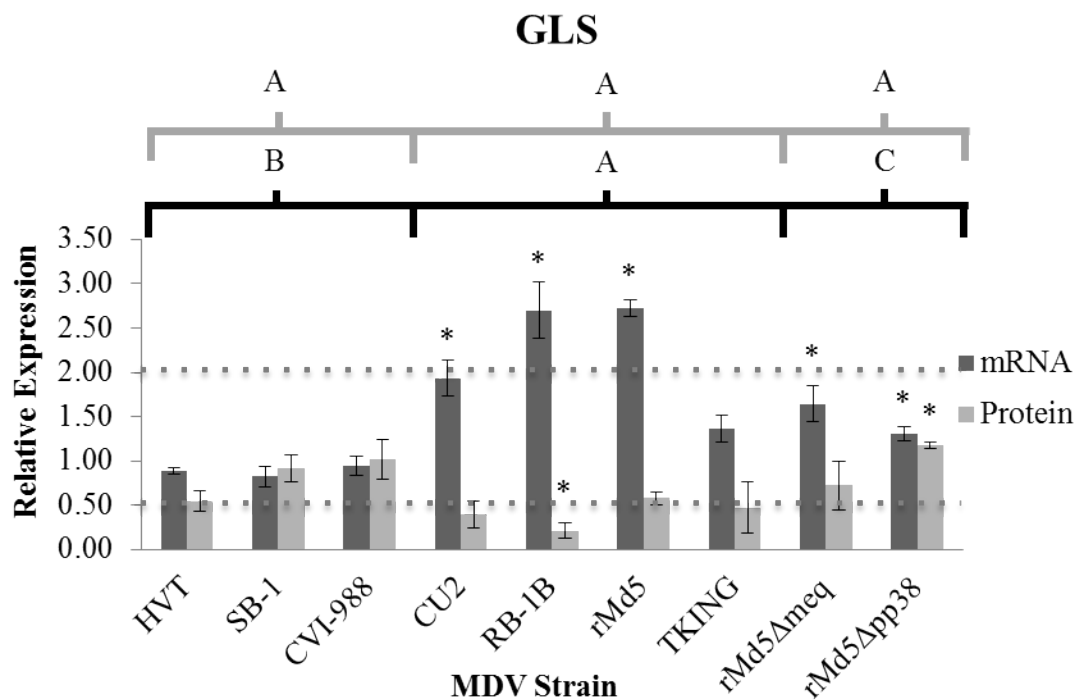


**Figure 3.16: Relative expression of GLS during cell culture MDV infection.** Data are expressed as mean relative expression of three samples (n=3) by strain with error bars representing the standard error. An asterisk denotes statistically significant differences from an average mock sample at the  $p < 0.05$  level, dotted lines represent a 2-fold change in expression as the biological significance, and the letters at the top represent a Tukey's HSD analysis for mRNA (black) and protein (gray) levels.

## **3.2 Targeted Proteomic Analysis: Western Blot Analysis**

### **3.2.1 Glycolytic Protein Expression During Infection with MDV**

To examine whether the Warburg effect could be detected at both the RNA and protein levels, western blot analysis was performed. Protein samples from the MDV strains used in this study (CU2, RB-1B, rMd5, TKING, HVT, SB-1, CVI-988, rMd5 $\Delta$ meq, and rMd5 $\Delta$ pp38) were separated by SDS-PAGE, blotted to a nitrocellulose membrane, and probed with the antibodies outlined in table 2.2. Band intensities were quantified using the ImageJ software supplied by the National Institutes of Health (NIH). The intensity values for all infected samples were compared to mock-infected band intensities to obtain relative band intensities, and then normalized to GAPDH values to account for variations in protein loading.

Figures A1 through A3 show the scanned Western blot bands corresponding to the predicted size of the protein product. Figures 3.1-3.6 and 3.14-3.16 show the normalized, relative band intensities. Despite some significant differences in glycolytic gene expression at the RNA level, there were very few differences observed however, at the protein level by this method. Infection with RB-1B, an oncogenic MDV, resulted in significant down regulation of the HIF-1 $\alpha$  transcription factor. All other proteins of interest showed no biologically significant change in expression during infection with oncogenic MDV.

Again, infection with vaccine and recombinant MDV strains showed little significant changes in protein expression. Infection with HVT resulted in decreased SLC2A1 protein which infection with the recombinant strains, rMd5 $\Delta$ meq and rMd5 $\Delta$ pp38, resulted in significantly decreased levels of SLC16A3 and HIF-1 $\alpha$  respectively. Although of questionable biological significance (less than a 2-fold

change in expression), the proteins HK2, LDHA, and SLC16A3 were slightly, yet statistically significantly up-regulated in cells infected with the MDV vaccine strains (HVT, SB-1, and CVI-988). These results (Figures 3.3, 3.5, and 3.6 respectively) are accompanied by a Tukey's HSD analysis which confirms this observation. Furthermore, this analysis showed no significant difference in SLC2A1 expression across strain groups, and a statistically significant increase in HIF-1 $\alpha$  expression during recombinant strain infection.

### **3.2.2 Glutaminolytic Protein Expression During Cell Culture MDV Infection**

Relative protein expression for the three glutaminolytic proteins tested (SLC1A4, SLC7A5, and GLS) are shown in figures 3.14 – 3.16. SLC1A4, a high affinity glutamate and neutral amino acid transporter, was down-regulated at the protein level in three of the four oncogenic strains (CU2, RB-1B, and TKING) and up-regulated during infection with rMd5 $\Delta$ pp38 (Figure 3.14). While infection with MDV showed no significant change in SLC7A5 expression, infection with RB-1B resulted in apparent decreased GLS expression.

Of the virus-infections showing biologically-significant increases in protein expression, rMd5 $\Delta$ pp38 infected cells showed increased HIF-1 $\alpha$  and SLC1A4 expression when compared to rMd5 and rMd5 $\Delta$ meq infected cells. These data were in stark contrast to the qRT-PCR data (Figures 3.1 – 3.6 and 3.14 – 3.16), which showed rMd5 expression to be higher for most of the genes tested compared to the two deletion mutants (rMd5 $\Delta$ meq and rMd5 $\Delta$ pp38). The one exception was PDK1 expression, which was higher in the recombinant MDV-infected cells. Also of interest was the correlation of increased HIF-1 $\alpha$  expression at the protein level in rMd5 $\Delta$ pp38 infected cells and one HIF-1 $\alpha$  inducible gene, PDK1 (Figure 3.4).

### **3.2.3 Direct Comparison of Transcriptional and Translational Profiles.**

A heat diagram analysis of RNA and protein expression (Figures 3.17 – 3.19) showed essentially no correlation between transcriptional (Figure 3.17) and protein expression (Figure 3.18) for any of the infections tested. Furthermore, using a biologically significant cutoff of a 2-fold change in relative expression left little significant change in protein expression during infection when compared to the fairly significant changes seen in mRNA expression (Figures 3.18 and 3.17 respectively).

Virus → Gene	HVT	SB-1	CVI-988	CU-2	RB-1B	rMd5	rMd5Δmeq	rMd5Δpp38	TKING
Glycolysis									
HIF-1α	Yellow	Yellow	Yellow	Red	Red	Red	Light Green	Light Green	Light Red
SLC2A1	Yellow	Yellow	Yellow	Light Red	Light Red	Yellow	Light Green	Light Green	Yellow
HK2	Yellow	Yellow	Light Red	Light Red	Red	Light Red	Yellow	Yellow	Yellow
PDK1	Yellow	Yellow	Yellow	Yellow	Yellow	Yellow	Yellow	Yellow	Yellow
LDHA	Yellow	Yellow	Yellow	Light Red	Light Red	Yellow	Yellow	Yellow	Yellow
SLC16A3	Yellow	Yellow	Yellow	Red	Red	Light Red	Light Green	Light Green	Red
Glutaminolysis									
SLC1A4	Yellow	Yellow	Yellow	Yellow	Yellow	Yellow	Yellow	Light Green	Yellow
SLC7A5	Light Green	Yellow	Yellow	Red	Yellow	Yellow	Light Green	Light Green	Red
GLS	Yellow	Yellow	Yellow	Light Red	Red	Red	Yellow	Yellow	Yellow
2-fold <	~2-fold <	~1	~2-fold >	2-fold >					
Bright Green	Light Green	Yellow	Light Red	Red					

**Figure 3.17 Heat summary of transcriptional expression during MDV infection.** Bright green denotes a greater than 2-fold decrease in relative expression where bright red denotes a greater than 2-fold increase in relative expression.

Virus → Gene	HVT	SB-1	CVI-988	CU-2	RB-1B	rMd5	rMd5Δmeq	rMd5Δpp38	TKING
Glycolysis									
HIF-1α	Yellow	Yellow	Yellow	Yellow	Light Green	Yellow	Light Red	Bright Red	Yellow
SLC2A1	Light Green	Yellow	Yellow	Yellow	Yellow	Yellow	Yellow	Yellow	Yellow
HK2	Yellow	Yellow	Yellow	Yellow	Yellow	Light Green	Light Green	Yellow	Yellow
LDHA	Yellow	Yellow	Yellow	Yellow	Light Green	Yellow	Yellow	Yellow	Light Green
SLC16A3	Yellow	Yellow	Yellow	Yellow	Yellow	Light Green	Yellow	Light Green	Yellow
Glutaminolysis									
SLC1A4	Yellow	Yellow	Yellow	Light Green	Bright Green	Yellow	Yellow	Light Red	Light Green
SLC7A5	Yellow	Yellow	Yellow	Yellow	Yellow	Yellow	Light Green	Yellow	Yellow
GLS	Yellow	Yellow	Yellow	Light Green	Light Green	Yellow	Yellow	Yellow	Light Green
<b>2-fold &lt;</b>	<b>~2-fold &lt;</b>	<b>~1</b>	<b>~2-fold &gt;</b>	<b>2-fold &gt;</b>					
Bright Green	Light Green	Yellow	Light Red	Bright Red					

**Figure 3.18 Heat summary of protein expression during MDV infection.** Bright green denotes a greater than 2-fold decrease in relative expression where bright red denotes a greater than 2-fold increase in relative expression.

Virus → Gene	TKING CEF mRNA	TKING CEF Protein	TKING Spleen Tumor
Glycolysis			
HIF-1 $\alpha$			
SLC2A1			
LDHA			
SLC16A3			
Glutaminolysis			
SLC7A5			
GLS			
<b>2-fold &lt;</b>	<b>~2-fold &lt;</b>	<b>~1</b>	<b>~2-fold &gt;</b>

**Figure 3.19 Heat Summary of transcriptional and protein expression during TKING cell culture and transcriptional expression during TKING *in vivo* infection.** Bright green denotes a greater than 2-fold decrease in relative expression where bright red denotes a greater than 2-fold increase in relative expression.

## **Chapter 4**

### **DISCUSSION**

Marek's disease virus (MDV) rapidly induces T-cell lymphomas in susceptible chickens. While transformation of T-cells has been primarily associated with latent MDV infection, early cytolytic infection is thought to contribute to the susceptibility of the chicken to lymphoma development and progression. We therefore hypothesized that cellular energy metabolism would be modified to mimic the Warburg effect during lytic infection to fuel the increased energy demand associated with viral replication, assembly, and egress.

To test our hypothesis that oncogenic MDV infection induces the reprogramming of energy metabolism we quantitatively analyzed select metabolic gene expression changes during infection. This hallmark of cancer was previously identified in a multitude of human cancers and viral infections (32, 130). As no previous reports have addressed the analysis of MDV infection and energy reprogramming, we provide the first analysis of these pathways at the transcriptional and translational levels in the context of MDV replication in cell culture.

#### **4.1 Glycolytic Gene Expression of Uninfected, MDV-infected and MDV-transformed Spleen Cells**

During tumorigenesis, proliferating cell masses outgrow their blood supply and become hypoxic (16). This hypoxic condition invokes a cascade of metabolic changes known as the Warburg effect (49). The irregular pattern of cellular energy metabolism linked with the Warburg effect is highly correlated with the stabilization of the

Hypoxia-inducible factor alpha subunit (HIF-1 $\alpha$ ) (90). Cells under normoxic conditions degrade this subunit through the hydroxylation of its two proline residues, mediated by an oxygen dependent E3 ubiquitin ligase (52, 53). In the hypoxic microenvironment of tumors, hydroxylation does not occur and therefore, the hypoxia inducible factor complex (HIF) is stabilized and up-regulates genes associated with metabolism, angiogenesis and cell motility (16, 50, 59).

Our data suggest that infection of chicken embryo fibroblasts (CEFs) with oncogenic MDV-1 strains results in increased transcriptional expression of HIF-1 $\alpha$ . This increased level of expression was also found in splenic tumors of chickens infected with TKING, a vv+MDV strain known for inducing tumors with necrotic central foci. Common to both CEF and splenic tumor infection with TKING were the induction of GLUT1 (SLC2A1), HIF-1 $\alpha$ , MCT4 (SLC16A3) of the glycolytic pathway and SLC7A5 of the glutaminolytic pathway. At the transcriptional level, therefore, it appeared that both lytic (CEF) and latent (tumor) infections affected HIF-1 $\alpha$  expression similarly.

The induction of HIF-1 $\alpha$  in CEF was increased; however this increase was not statistically significant, nor was it corroborated at the protein level. This lack of significance could have been due to biological variability between samples. A Tukey's HSD analysis showed significantly higher levels of HIF-1 $\alpha$  expression during oncogenic MDV infection when compared with vaccine MDV infection. This may suggest that the ability of MDV to cause Marek's disease, but not its ability to infect cells, is responsible for the increased expression of HIF-1 $\alpha$ . Due to the fact that the cell culture infections used CEFs, cells that are not susceptible to transformation, the

changes in HIF-1 $\alpha$  expression are most likely due to the viral infection and not transformation or hypoxic conditions found in most tumors.

When up-regulated, the HIF1 complex is able to affect multiple pathways throughout the cell, the most profound of which is the glycolytic pathway (34). On the other hand, when the recombinant MDV strains, rMd5 $\Delta$ meq and rMd5 $\Delta$ pp38 were screened for changes in HIF-1 $\alpha$  expression, we found significant down-regulation at the transcriptional level. Down-regulation of this integral transcription factor would suggest an overall decrease in glycolytic function and furthermore suggests that Meq and pp38 may both be involved in the transcriptional regulation of these genes during latent/transforming and lytic infections, respectively, a phenomena previously described by Parcels *et al.* (84).

In most cases where HIF-1 $\alpha$  is up-regulated and the cells are exhibiting the Warburg effect, glycolytic function is greatly increased (68). Surprisingly, increased levels of glycolysis and pyruvate production seen during this effect do not correlate with an increased level of acetyl-CoA entering the mitochondria. This unexpected decrease in acetyl-CoA production and therefore expected decrease in TCA cycle function would lead to an eighteen-fold decrease in ATP production, a counterintuitive shift in energy metabolism (47). The energy deficit elicited by decreased ATP production is, in part, relieved through increasing glucose transport into the infected cells.

Our results show that infection with oncogenic MDV caused slight transcriptional up-regulation of SLC2A1, a major glucose transporter found in chickens. On the other hand, infection with vaccine strains of MDV resulted in no significant changes in gene expression. The difference between gene expression

during oncogenic and vaccine strain replication in CEF suggests that there may be properties of oncogenic MDV associated with increased glucose transport into the cells, and that these are inherent to lytic infection.

As noted above, expression of HIF-1 $\alpha$  and SLC2A1 was significantly decreased during infection with the rMd5 $\Delta$ Meq and rMd5 $\Delta$ pp38 strains. These data are consistent with decreased levels of glycolysis suggested by the decreased HIF-1 $\alpha$  expression.

Following transport into the cell, glucose is phosphorylated into glucose-6-phosphate by hexokinase 2 (HK2), a rate limiting step in glycolysis. At the transcript level HK2 transcription was increased ( $\geq 2$  fold) in CVI-988-, CU-2- RB-1B- and rMd5-infected cells. No such induction was seen in HVT-, SB-1-, rMd5 $\Delta$ Meq-, rMd5 $\Delta$ pp38- or TKING-infected cells. It is therefore difficult to correlate transcriptional expression of HK2 with virus pathotype. At the protein level, however, no such induction of HK2 was observed.

Glyceraldehyde-3-phosphate dehydrogenase (GAPDH), the enzyme responsible for the catabolic switch of glyceraldehyde-3-phosphate into D-glycerate-1,3-bisphosphate during glycolysis, has long been used as a stable housekeeping gene. The literature shows that this gene is regulated by the HIF-1 $\alpha$  transcription factor and therefore should be analyzed for stability before use as a housekeeping gene (34, 125). Our data showed a relatively stable expression of GAPDH during cell culture infection and increased expression in the tumor samples. The glycolytic step catalyzed by GAPDH requires large quantities of NAD<sup>+</sup> and therefore stresses highly proliferating cells to produce this substrate. Considering the fact that NAD<sup>+</sup> is a byproduct of

lactate production, one of the only ways to support growing  $\text{NAD}^+$  requirements is to increase lactate production (26).

Pyruvate produced in the concluding steps of glycolysis is normally converted into Acetyl-CoA and moved into the mitochondria for further processing. However, under the Warburg effect, most of the pyruvate being produced is shunted away from the mitochondria and catabolized into lactate by lactate dehydrogenase A (LDHA) (26). In addition to refueling levels of  $\text{NAD}^+$ , the production of lactate alleviates the growing pool of pyruvate being produced from increased levels of glycolysis (26, 34).

Based on our results, oncogenic MDVs slightly increased transcriptional expression of LDHA during the infection of CEF (Figure 3.5), and spleen tumors (Figure 3.14). As with the oncogenic MDV infection, increased expression of this gene has previously been associated with tumorigenesis through a host of different cancers such as pancreatic cancer, multiple myeloma, and esophageal carcinomas (39, 91, 123). At the protein level, however, LDHA was not induced as seen transcriptionally, and the vaccine strain CVI-988 showed the overall highest level of expression (Figure 3.22). This induced level of LDHA expression however, was just under 2 fold. Thus again, there appeared to be a lack of transcriptional and translational correlation.

Growing levels of intercellular lactate due to increased LDHA transcription cause increased stress on the cells. The pooling lactate is relieved through the action of the solute carrier family 16 member 3 transporter (SLC16A3). Its ability to export both lactate and hydrogen ions out of the cell is critical for highly proliferating cells that exhibit high levels of glycolysis (46, 79, 110). Our data suggest that at the transcriptional level, transport of lactate out of both CEFs and tumor cells is

significantly increased during oncogenic, but not non-oncogenic or attenuated MDV infection (Figure 3.6). Significantly higher in oncogenic strains, the transport of lactate and hydrogen ions into the extracellular space could be a contributing factor to decreased extracellular pH seen in multiple types of cancers (37, 104). In accordance with the other glycolytic genes discussed, increased SLC16A3 expression has been linked with increased HIF-1 $\alpha$  expression during infection and tumorigenesis (109). Furthermore, as seen in Figure 3.6, the expression of SLC16A3 is significantly decreased during infection with rMd5 $\Delta$ Meq and rMd5 $\Delta$ pp38. At the protein level, only the decrease of SLC16A3 expression in rMd5 $\Delta$ Meq cells was consistent with the observed transcriptional decrease (Figure 3.23).

The ability of pyruvate dehydrogenase kinase (PDK1) to down-regulate the mitochondrial pyruvate dehydrogenase complex is critical for a multitude of cancers due to its ability to decrease the movement of pyruvate into Acetyl-CoA, effectively shunting pyruvate towards lactate production. (34, 95, 110). Despite this, our data show that MDV infection has no effect on the levels of PDK1 expression across almost all strains tested at the transcript level. A near two-fold transcriptional increase was noted for rMd5 $\Delta$ pp38-infected cells, but its significance was not clear and PDK1 expression was not tested at the protein level.

#### **4.2 Glutaminolytic Gene Expression of Uninfected, MDV-infected and MDV-transformed Spleen Cells**

The major glycolytic transcription factor, HIF-1 $\alpha$ , showed increased transcriptional expression during *in vivo* MDV infection in our study, consistent with an association of MDV infection and the Warburg effect. Similar to the ability of HIF-1 $\alpha$  to act as a glycolytic transcription factor, the gene c-Myc can act as a

glutaminolytic transcription factor (75). This gene, shown to regulate viral telomerase (vTR) expression in MDV-transformed cells and to act as an oncogene in times of overexpression, shares many downstream transcription targets with HIF-1 $\alpha$  (100, 124).

The documented role of c-Myc in glycolysis and glutaminolysis regulation during infection, and its ability to regulate gene transcription during MDV infection made it a good candidate gene (75, 100). Upon testing c-myc for changes in transcriptional expression during MDV infection, we saw no significant differences when compared to mock infected cells (data not shown). We did not test the expression of c-Myc at the protein level, however c-Myc was not found to be upregulated in MDV lymphoma CD30hi cells (17).

Despite the lack of evidence for c-Myc induction during MDV infection, the pathway of glutaminolysis was still investigated due to its importance as a basic metabolic process in both healthy and tumorigenic cells (116, 130). Our data show that the first step of this process, the transition of glutamine into glutamate by glutaminase is significantly increased during cell culture infection with RB-1B and rMd5 strains, but not affected during *in vivo* infection. Furthermore, glutamine transport back out of the cell and essential amino acid transport into the cell, facilitated by the bi-directional SLC7A5 transporter was increased transcriptionally during oncogenic infection in both cell culture and *in vivo* samples, and significantly decreased during infection with rMd5 $\Delta$ meq and rMd5 $\Delta$ pp38. However, these transcriptional differences were not consistent with our Western blot analysis for the SLC7A5 protein, which showed only a down-regulation in rMd5 $\Delta$ meq-infected cells (Figures 3.12 and 3.25).

Finally, expression of the neutral amino acid transporter, SLC1A4, while not increased during oncogenic MDV infection, did show a transcriptional decrease during recombinant MDV infection. However, SLC1A4 protein expression was significantly increased during infection with rMd5 $\Delta$ pp38, suggesting that pp38 of oncogenic MDV-1 strains may be involved in the regulation of this pathway.

Additionally, the transcriptional increase of SLC7A5, and ostensibly its accumulation in the membranes of cells, actively induces leucine induction into the cell. Due to leucine's ability to co-activate glutaminolysis, the increased expression of the SLC7A5 transporter can act as a positive "feed-forward" activation pathway (116, 130). Furthermore, the increased TCA cycle activation made possible through these changes may help alleviate the decreased ATP production brought on by the Warburg effect, a growing trend linked with tumor growth in multiple cancers (67, 103, 108). Comparatively, our data show that oncogenic strains of MDV harbor a distinct glutaminolytic advantage over the vaccine strains, at least at the transcript level.

In addition to meeting increased energy requirements of highly proliferating tumor cells and MDV-infected CEFs, as mentioned previously, the up-regulation of glycolysis and glutaminolysis provides these cells with essential macromolecules such as lipids, proteins, and nucleic acids for cellular proliferation (13). Even though during the Warburg effect, eighty-five percent of cellular pyruvate is shunted towards lactate production, as supported by increased LDHA levels during MDV infection, the remaining pyruvate is catabolized into Acetyl-CoA (110). These stocks, along with the  $\alpha$ -ketoglutarate being produced during late glutaminolysis fuel the TCA cycle and allow for the production of various metabolites. These essential metabolites are used in downstream pathways such as lipid, amino acid, and pyruvate synthesis (110).

Interestingly, it has been found that MDV infection induces lipid accumulation both *in vivo* and cell culture models, giving further evidence to this idea of the Warburg effect during MDV infection (38, 45). These actions make the mitochondria act not only as an energy producing organelle, but also as a biosynthetic center (56).

### **4.3 Discrepancy Between Transcript and Protein Expression Values**

The increased transcription of some of the glycolytic and glutaminolytic genes tested during oncogenic MDV infection sheds light on the possible cellular modifications that lead to tumorigenesis in infected chickens. While some of these findings seem to be of biological significance, as we have seen in our data, they may not directly confer a change at the protein level. This lack of correlation between mRNA and protein levels has been well documented (112, 126).

This discrepancy could be due to either technical- or biological-based reasons. From a technical standpoint, the western blotting protocol used may not have been optimal for the detection of membrane channel proteins. Previous studies have reported difficulty analyzing transmembrane (TM) proteins due to their usually high molecular weights or their relative insolubility (105). This inherent insolubility is attributed to the hydrophobic regions of these proteins found within the lipid bilayer of most cells (76). When the membrane is disrupted during protein extraction, these hydrophobic regions may aggregate together and cause the formation of an insoluble fraction (105).

Alternatively, a more biologically-based reason for the disparity observed between transcript and protein levels comes from the use of chicken embryo fibroblasts (CEF) as the target cell. CEF are not susceptible to MDV transformation and therefore they only support lytic MDV replication. Therefore, one possibility is

that post-translational modification inhibits increased metabolic protein expression during lytic infection, but during latent infection these proteins would have been easily detected. Much like in our study, it is assumed that these metabolic changes adapt the infected cells for tumorigenesis.

Whether the discrepancy between transcript and protein expression seen in our study stems from technical or biological causes, there exists methods that can be employed to minimize these differences. In order to alleviate the problems of difficulty in solubilizing membrane proteins or increased antibody background during western blotting, mass spectrometry would provide a quantitative, and specific alternative to verify qRT-PCR results (2). In addition, the *in situ* staining of infected cells by immunofluorescence analysis would allow the direct comparison of MDV-infected and uninfected cells through quantitative measurement of fluorescence intensity.

## Chapter 5

### CONCLUSIONS AND FUTURE DIRECTION

#### 5.1 Conclusions

On the transcriptome level, this study has shed light on the underlying metabolic modifications taking place during Marek's disease virus infection. While there was no apparent correlation between virulence and gene modulation, there were significant differences between oncogenic and vaccine strain infection.

Conversely, infection with MDV vaccine strains resulted in either decreased expression or no significant change in expression. These data suggest the link between oncogenicity and the Warburg effect. Interestingly, when infected with recombinant MDV strains that are missing either the major MDV oncogene (meq), or the lytic regulatory gene pp38, most glycolytic genes were significantly down-regulated.

The western blot analysis we performed resulted in little significant changes in glycolytic and glutaminolytic protein expression levels when comparing Marek's disease virus (MDV) infected CEF to mock infected CEF. Furthermore, the significant changes in protein expression we did observe did not correspond with the previously stated changes in mRNA expression values seen during infection. Therefore, the western blot analysis is not able to validate our transcriptomic data. This result may be attributed to either technical or biological differences observed between transcription and translation, or that MDV does not affect glycolytic or glutaminolytic pathways of CEF during lytic infection (14, 70).

## 5.2 Future Direction for this Research

While there exists little correlation between transcript and protein expression levels in this study, there are several directions for the continuation of this work. First, and foremost, the effect of MDV lytic, latent and transforming infections on glucose and glutamine utilization and microenvironment pH needs to be established. The only evidence we have so far is that MDV-transformed T-cell lines require supplementation with glucose and L-glutamine, among other nutrients, for propagation in cell culture and as these cells proliferate, there is a pH drop as measured by a color change in phenol red containing base medium.

Second, in terms of a model for latency, our laboratory has established a model using the reticuloendotheliosis virus (REV)-transformed, CU91 line (8, 9). This cell line was used to model oncogenic, vaccine, and recombinant MDV latent infection (8, 9), as MDV strains infect this CD4<sup>+</sup> cell line and establish latency. The issue with this model is that the contribution of v-Rel transformation may overshadow any MDV-mediated effects.

Third, in terms of identifying the Warburg effect in MDV-transformed cells, tumor cells could be analyzed by RNAseq and mass spectrometry directly *ex vivo*, as has been performed by Shack and Burgess, for CD30<sup>hi</sup> and CD30<sup>lo</sup> expressing tumor cells (98).

## REFERENCES

1. **Acheson NH**. 2011. Introduction to Virology, p 2-17. *In: Fundamentals of Molecular Virology*. 2 ed.
2. **Aebersold R, Burlingame AL, Bradshaw RA**. 2013. Western Blots vs. SRM Assays: Time to turn the tables? *Molecular & Cellular Proteomics*.
3. **Afonso CL, Tulman ER, Lu Z, Zsak L, Rock DL, Kutish GF**. 2001. The genome of turkey herpesvirus. *Journal of Virology* **75**:p 971-978.
4. **Ajithdoss DK, Reddy SM, Suchodolski PF, Lee LF, Kung HJ, Lupiani B**. 2009. In vitro characterization of the Meq proteins of Marek's disease virus vaccine strain CVI-988. *Virus Research* **142**:p 57-67.
5. **Alberts B, Johnson A, Lewis J, Raff M, Roberts K, Walter P**. 2008. Cell chemistry and biosynthesis, p 45-124. *In: Molecular Biology of the Cell*. 5 ed. Garland Science, New York, NY.
6. **Aledo JC**. 2004. Glutamine breakdown in rapidly dividing cells: waste or investment? *BioEssays* **26**:p 778-785.
7. **Arriza JL, Kavanaugh MP, Fairman WA, Wu YN, Murdoch GH, North RA, Amara SG**. 1993. Cloning and expression of a human neutral amino acid transporter with structural similarity to the glutamate transporter gene family. *Journal of Biological Chemistry* **268**:p 15329-15332.
8. **Arumugaswami V, Kumar PM, Konjufca V, Dienglewicz RL, Reddy SM, Parcels MS**. 2009. Latency of Marek's disease virus (MDV) in a reticuloendotheliosis virus-transformed T-cell line. I: Uptake and structure of the latent MDV genome. *Avian Diseases Digest* **4**:p e1.
9. **Arumugaswami V, Kumar PM, Konjufca V, Dienglewicz RL, Reddy SM, Parcels MS**. 2009. Latency of Marek's disease virus (MDV) in a reticuloendotheliosis virus-transformed T-cell line. II: Expression of the latent MDV genome. *Avian Diseases Digest* **4**:p e2. doi:doi: 10.1637/8862.1.

10. **Atkins K, Read A, Savill N, Renz K, Walkden-Brown S, Woolhouse M.** 2011. Modelling Marek's Disease Virus (MDV) infection: parameter estimates for mortality rate and infectiousness. *BMC Veterinary Research* **7**:p 70. doi:10.1186/1746-6148-7-70.
11. **Baigent SJ, Ross LJ, Davison TF.** 1998. Differential susceptibility to Marek's disease is associated with differences in number, but not phenotype or location, of pp38+ lymphocytes. *Journal of General Virology* **79**:p 2795-2802.
12. **Barrow A, Venugopal K.** 1999. Molecular characteristics of very virulent European MDV isolates. *Acta Virologica* **43**:p 90-93.
13. **Bauer DE, Hatzivassiliou G, Zhao F, Andreadis C, Thompson CB.** 2005. ATP citrate lyase is an important component of cell growth and transformation. *Oncogene* **24**:p 6314-6322.
14. **Berg J, Tymoczko JL, Stryer L.** 2002. Section 28.2, Eukaryotic transcription and translation are separated in space and time., *In: Biochemistry.* 5th edition ed. Freeman, W H, New York.
15. **Boer GF, Groenendal JE, Boerrigter HM, Kok GL, Pol JMA.** 1986. Protective efficacy of Marek's disease virus (MDV) CVI-988 CEF65 clone C against challenge infection with three very virulent MDV strains. *Avian Diseases* **30**:p 276-283.
16. **Brown JM, Giaccia AJ.** 1998. The unique physiology of solid tumors: opportunities (and problems) for cancer therapy. *Cancer Research* **58**:p 1408-1416.
17. **Burgess SC, Young JR, Baaten BJG, Hunt L, Ross LNJ, Parcels MS, Kumar PM, Tregaskes CA, Lee LF, Davison TF.** 2004. Marek's disease is a natural model for lymphomas overexpressing Hodgkin's disease antigen (CD30). *Proceedings of the National Academy of Sciences of the United States of America* **101**:p 13879-13884.
18. **Calnek BW, Schat KA, Peckham MC, Fabricant J.** 1983. Field trials with a bivalent vaccine (HVT and SB-1) against Marek's disease. *Avian Disease* **27**:p 844-849.
19. **Calnek BW.** 2001. Pathogenesis of Marek's disease virus infection, p 25-55. *In: Hirai K (ed), Marek's Disease.* 255 ed. Springer Berlin Heidelberg.

20. **Calnek BW, Adldinger HK, Kahn DE.** 1970. Feather follicle epithelium: A source of enveloped and infectious cell-free herpesvirus from Marek's disease. *Avian Diseases* **14**:p 219-233.
21. **Calnek B, Harris R, Buscaqlia C, Schat K, Lucio B.** 1998. Relationship between the immunosuppressive potential and the pathotype of Marek's disease virus isolates. *Avian Diseases* **42**:p 124-132.
22. **Camarena V, Kobayashi M, Kim JY, Roehm P, Perez R, Gardner J, Wilson AC, Mohr I, Chao MV.** 2010. Nature and duration of growth factor signaling through receptor tyrosine kinases regulates HSV-1 latency in neurons. *Cell Host & Microbe* **8**:p 320-330. doi:doi:10.1016/j.chom.2010.09.007.
23. **Cebrian J, Kaschka-Dierich C, Berthelot N, Sheldrick P.** 1982. Inverted repeat nucleotide sequences in the genomes of Marek disease virus and the herpesvirus of the turkey. *Proceedings of the National Academy of Sciences* **79**:p 555-558.
24. **Chambers JW, Maguire TG, Alwine JC.** 2010. Glutamine metabolism is essential for human cytomegalovirus infection. *Journal of Virology* **84**:p 1867-1873.
25. **CHANG KS, OHASHI K, ONUMA M.** 2002. Diversity (polymorphism) of the meq gene in the attenuated Marek's disease virus (MDV) serotype 1 and MDV-transformed cell lines. *Journal of Veterinary Medical Science* **64**:p 1097-1101.
26. **Chiarugi A, Dolle C, Felici R, Ziegler M.** 2011. The NAD metabolome [mdash] a key determinant of cancer cell biology. *Nat Rev Cancer* **12**:p 741-752.
27. **Churchill AE, Biggs PM.** 1967. Agent of Marek's disease in tissue culture. *Nature* **215**:p 528-530.
28. **Cooper G.** 2000. Metabolic energy, *In: The Cell: A Molecular Approach*. 2 ed. Sinauer Associates, Sunderland, MA.
29. **Cui ZZ, Lee LF, Liu JL, Kung HJ.** 1991. Structural analysis and transcriptional mapping of the Marek's disease virus gene encoding pp38, an antigen associated with transformed cells. *Journal of Virology* **65**:p 6509-6515.
30. **Dang CV.** 2010. Glutaminolysis: Supplying carbon or nitrogen or both for cancer cells *Cell Cycle* **9**:p 3914-3916.

31. **Darekar S, Georgiou K, Yurchenko M, Yenamandra SP, Chachami G, Simos G, Klein G, Kashuba E.** 2012. Epstein-Barr Virus immortalization of human B-cells leads to stabilization of hypoxia-induced factor 1 alpha, congruent with the Warburg effect. *PLoS ONE* **7**:p e42072. doi:doi:10.1371/journal.pone.0042072.
32. **Delgado T, Carroll PA, Punjabi AS, Margineantu D, Hockenbery DM, Lagunoff M.** 2010. Induction of the Warburg effect by Kaposi's sarcoma herpesvirus is required for the maintenance of latently infected endothelial cells. *Proceedings of the National Academy of Sciences*.
33. **Deng X, Li X, Shen Y, Qiu Y, Shi Z, Shao D, Jin Y, Chen H, Ding C, Li L, Chen P, Ma Z.** 2010. The Meq oncoprotein of Marek's disease virus interacts with p53 and inhibits its transcriptional and apoptotic activities. *Virology Journal* **7**:p 348. doi:10.1186/1743-422X-7-348.
34. **Denko NC.** 2008. Hypoxia, HIF1 and glucose metabolism in the solid tumour. *Nat Rev Cancer* **8**:p 705-713. doi:10.1038/nrc2468.
35. **Dunn J.** 2013. Neoplasms: Marek's disease in poultry, *In*: Aiello SE, Moses MA (eds), *The Merck Veterinary Manual*. 10 ed. Merck Publishing Group.
36. **Dunn JR, Silva RF.** 2012. Ability of MEQ-deleted MDV vaccine candidates to adversely affect lymphoid organs and chicken weight gain. *Avian Diseases* **56**:p 494-500. doi:doi: 10.1637/10062-011812-Reg.1.
37. **Estrella V, Chen T, Lloyd M, Wojtkowiak J, Cornell HH, Ibrahim-Hashim A, Bailey K, Balagurunathan Y, Rothberg JM, Sloane BF, Johnson J, Gatenby RA, Gillies RJ.** 2013. Acidity generated by the tumor microenvironment drives local invasion. *Cancer Research* **73**:p 1524-1535.
38. **Fabricant C, Hajjar D, Minick C, Fabricant J.** 1981. Herpesvirus infection enhances cholesterol and cholesteryl ester accumulation in cultured arterial smooth muscle cells. *American Journal of Pathology* **105**:p 176-184.
39. **Fujiwara S, Kawano Y, Yuki H, Okuno Y, Nosaka K, Mitsuya H, Hata H.** 2013. PDK1 inhibition is a novel therapeutic target in multiple myeloma. *British Journal of Cancer* **108**:p 170-178.
40. **Fukuchi K, Sudo M, Lee YS, Tanaka A, Nonoyama M.** 1984. Structure of Marek's disease virus DNA: detailed restriction enzyme map. *Journal of Virology* **51**:p 102-109.

41. **Gimeno IM, Witter RL, Hunt HD, Reddy SM, Lee LF, Silva RF.** 2005. The pp38 gene of Marek's disease virus (MDV) is necessary for cytolytic infection of B cells and maintenance of the transformed state but not for cytolytic infection of the feather follicle epithelium and horizontal spread of MDV. *Journal of Virology* **79**:p 4545-4549.
42. **Gong Z, Zhang L, Wang J, Chen L, Shan H, Wang Z, Ma H.** 2013. Isolation and analysis of a very virulent Marek's disease virus strain in China. *Virology Journal* **10**:p 155. doi:10.1186/1743-422X-10-155.
43. **Gonnella R, Santarelli R, Farina A, Granato M, D'Orazi G, Faggioni A, Cirone M.** 2013. Kaposi sarcoma associated herpesvirus (KSHV) induces AKT hyperphosphorylation, bortezomib-resistance and GLUT-1 plasma membrane exposure in THP-1 monocytic cell line. *Journal of Experimental & Clinical Cancer Research* **32**:p 79. doi:10.1186/1756-9966-32-79.
44. **Gould GW, Bell GI.** 1990. Facilitative glucose transporters: an expanding family. *Trends in Biochemical Sciences* **15**:p 18-23.
45. **Hajjar D, Fabricant C, Minick C, Fabricant J.** 1986. Virus-induced atherosclerosis. Herpesvirus infection alters aortic cholesterol metabolism and accumulation. *American Journal of Pathology* **122**:p 62-70.
46. **Halestrap A, Price N.** 1999. The proton-linked monocarboxylate transporter (MCT) family: structure, function and regulation. *Biochemical Journal* **343 Pt 2**:p 281-299.
47. **Hanahan D, Weinberg R.** Hallmarks of cancer: The next generation. *Cell* **144**(5), p 646-674. 3-4-2011.
48. **Haq K, Fear T, Ibraheem A, Abdul-Careem MF, Sharif S.** 2011. Influence of vaccination with CVI-988/Rispens on load and replication of a very virulent Marek's disease virus strain in feathers of chickens. *Avian Pathology* **41**:p 69-75. doi:doi: 10.1080/03079457.2011.640304.
49. **Hockel M, Vaupel P.** Tumor hypoxia: Definitions and current clinical, biologic, and molecular aspects. *Journal of the National Cancer Institute* **93**(4), p 266-276. 2-21-2001.
50. **Hu CJ, Wang LY, Chodosh LA, Keith B, Simon MC.** 2003. Differential roles of hypoxia-inducible factor 1a (HIF-1a) and HIF-2a in hypoxic gene regulation. *Molecular and Cellular Biology* **23**:p 9361-9374.

51. **Islam AFMF, Wong CW, Walkden-Brown SW, Colditz IG, Arzey KE, Groves PJ.** 2002. Immunosuppressive effects of Marek's disease virus (MDV) and herpesvirus of turkeys (HVT) in broiler chickens and the protective effect of HVT vaccination against MDV challenge. *Avian Pathology* **31**:p 449-461. doi:doi: 10.1080/0307945021000005824.
52. **Ivan M, Kondo K, Yang H, Kim W, Valiando J, Ohh M, Salic A, Asara JM, Lane WS, Kaelin J.** 2001. HIF-1a targeted for VHL-mediated destruction by proline hydroxylation: Implications for O<sub>2</sub> sensing. *Science* **292**:p 464-468.
53. **Jaakkola P, Mole DR, Tian YM, Wilson MI, Gielbert J, Gaskell SJ, Kriegsheim Av, Hebestreit HF, Mukherji M, Schofield CJ, Maxwell PH, Pugh C, Ratcliffe P.** 2001. Targeting of HIF-1a to the von Hippel-Lindau ubiquitylation complex by O<sub>2</sub>-regulated prolyl hydroxylation. *Science* **292**:p 468-472.
54. **Jones D, Lee L, Liu JL, Kung HJ, Tillotson JK.** 1992. Marek disease virus encodes a basic-leucine zipper gene resembling the fos/jun oncogenes that is highly expressed in lymphoblastoid tumors. *Proceedings of the National Academy of Sciences* **89**:p 4042-4046.
55. **Jones JO, Arvin AM.** 2003. Microarray analysis of host cell gene transcription in response to Varicella-Zoster Virus infection of human T cells and fibroblasts in vitro and SCIDhu skin xenografts in vivo. *Journal of Virology* **77**:p 1268-1280.
56. **Jones RG, Thompson CB.** 2009. Tumor suppressors and cell metabolism: a recipe for cancer growth. *Genes & Development* **23**:p 537-548.
57. **Kahn CM, Scott Line.** 2010. Marek's Disease, *In: The Merck Veterinary Manual.*
58. **Korotchkina LG, Patel MS.** 2001. Site specificity of four pyruvate dehydrogenase kinase isoenzymes toward the three phosphorylation sites of human pyruvate dehydrogenase. *Journal of Biological Chemistry* **276**:p 37223-37229.
59. **Koukourakis MI, Giatromanolaki A, Sivridis E, Simopoulos C, Turley H, Talks K, Gatter KC, Harris AL.** 2002. Hypoxia-inducible factor (HIF1A and HIF2A), angiogenesis, and chemoradiotherapy outcome of squamous cell head-and-neck cancer. *International Journal of Radiation Oncology\*Biology\*Physics* **53**:p 1192-1202.

60. **Kung H-J**. 2004. Chapter 4: Marek's disease virus oncogenicity: Molecular mechanisms, *In*: Davison TF, Nair V (eds), Marek's Disease: An Evolving Problem.
61. **Laurent AM, Madjar JJ, Greco A**. 1998. Translational control of viral and host protein synthesis during the course of herpes simplex virus type 1 infection: evidence that initiation of translation is the limiting step. *Journal of General Virology* **79**:p 2765-2775.
62. **Lee LF, Wu P, Sui D, Ren D, Kamil J, Kung HJ, Witter RL**. 2000. The complete unique long sequence and the overall genomic organization of the GA strain of Marek's disease virus. *Proceedings of the National Academy of Sciences* **97**:p 6091-6096.
63. **Levy AM, Gilad O, Xia L, Izumiya Y, Choi J, Tsalenko A, Yakhini Z, Witter R, Lee L, Cardona CJ, Kung HJ**. 2005. Marek's disease virus Meq transforms chicken cells via the v-Jun transcriptional cascade: A converging transforming pathway for avian oncoviruses. *Proceedings of the National Academy of Sciences of the United States of America* **102**:p 14831-14836.
64. **Li X, Jarosinski KW, Schat KA**. 2006. Expression of Marek's disease virus phosphorylated polypeptide pp38 produces splice variants and enhances metabolic activity. *Veterinary Microbiology* **117**:p 154-168.
65. **Lin J, Redies C**. 2012. Histological evidence: housekeeping genes beta-actin and GAPDH are of limited value for normalization of gene expression. *Dev Genes Evol* **222**:p 369-376.
66. **Liu JL, Ye Y, Qian Z, Qian Y, Templeton DJ, Lee LF, Kung HJ**. 1999. Functional interactions between herpesvirus oncoprotein Meq and cell cycle regulator CDK2. *Journal of Virology* **73**:p 4208-4219.
67. **Lobo C, Ruiz-Bellido MA, Aledo JC, Marquez, Nunez De Castro, Alonso FJ**. 2013. Inhibition of glutaminase expression by antisense mRNA decreases growth and tumourigenicity of tumour cells. *Biochemical Journal* **358**:p 257-261.
68. **Lu H, Forbes RA, Verma A**. 2002. Hypoxia-inducible factor 1 activation by aerobic glycolysis implicates the Warburg effect in carcinogenesis. *Journal of Biological Chemistry* **277**:p 23111-23115.

69. **Lupiani B, Lee LF, Cui X, Gimeno I, Anderson A, Morgan RW, Silva RF, Witter RL, Kung HJ, Reddy SM.** 2004. Marek's disease virus-encoded Meq gene is involved in transformation of lymphocytes but is dispensable for replication. *Proceedings of the National Academy of Sciences of the United States of America* **101**:p 11815-11820.
70. **Maier T, Guell M, Serrano L.** 2009. Correlation of mRNA and protein in complex biological samples. *FEBS Letters* **583**:p 3966-3973.
71. **Marek J.** 1907. Multiple Nervenentzündung (Polyneuritis) bei Hühnern. *Dtsch. Tierärztl. Wochenschr* **15**:p 417-421.
72. **Martin JA, Wang Z.** 2011. Next-generation transcriptome assembly. *Nat Rev Genet* **12**:p 671-682. doi:10.1038/nrg3068.
73. **Mathupala SP, Heese C, Pedersen PL.** 1997. Glucose Catabolism in Cancer Cells: The type II hexokinase promoter contains functionally active response elements for the tumor suppressor p53. *Journal of Biological Chemistry* **272**:p 22776-22780.
74. **McFarlane S, Nicholl MJ, Sutherland JS, Preston CM.** 2011. Interaction of the human cytomegalovirus particle with the host cell induces hypoxia-inducible factor 1 alpha. *Virology* **414**:p 83-90.
75. **Morrish F, Isern N, Sadilek M, Jeffrey M, Hockenbery DM.** 2009. c-Myc activates multiple metabolic networks to generate substrates for cell-cycle entry. *Oncogene* **28**:p 2485-2491.
76. **Nelson DL, Cox MM.** 2008. Chapter 11: Biological membranes and transport, p 371-418. *In: Lehninger Principles of Biochemistry*. Fifth ed. W. H. Freeman.
77. **Nelson DL, Cox MM.** 2008. Chapter 14: Glycolysis, gluconeogenesis, and the pentos phosphate pathway, *In: Lehninger Principles of Biochemistry*. Fifth ed. W. H. Freeman.
78. **Okazaki W, Purchase HG, Burmester BR.** 1970. Protection against Marek's disease by vaccination with a herpesvirus of turkeys. *Avian Diseases* **14**:p 413-429.
79. **Ord J, Streeter E, Roberts I, Cranston D, Harris A.** 2005. Comparison of hypoxia transcriptome in vitro with in vivo gene expression in human bladder cancer. *Br J Cancer* **93**:p 346-354.

80. **Osterrieder N, Kamil JP, Schumacher D, Tischer BK, Trapp S.** 2006. Marek's disease virus: from miasma to model. *Nat Rev Micro* **4**:p 283-294. doi:10.1038/nrmicro1382.
81. **Pappenheimer AM, Dunn LC, Cone V.** 1929. Studies on fowl paralysis (neurolymphomatosis gallinarum): I. clinical features and pathology. *The Journal of Experimental Medicine* **49**:p 63-86.
82. **Parcells MS, Arumugaswami V, Prigge JT, Pandya K, Dienglewicz RL.** 2003. Marek's disease virus reactivation from latency: changes in gene expression at the origin of replication. *Poultry Science* **82**:p 893-898.
83. **Parcells M, Burgess S.** 2008. Immunological aspects of Marek's disease virus (MDV)-induced lymphoma progression, p 169-191. *In*: Kaiser H, Nasir A (eds), *Selected Aspects of Cancer Progression: Metastasis, Apoptosis and Immune Response*. 11 ed. Springer Netherlands.
84. **Parcells M, Arumugaswami V, Prigge J, Pandya K, Dienglewicz R.** 2003. Marek's disease virus reactivation from latency: changes in gene expression at the origin of replication. *Poultry Science* **82**:p 893-898.
85. **Piepenbrink M, Li X, OConnell P, Schat K.** 2009. Marek's disease virus phosphorylated polypeptide pp38 alters transcription rates of mitochondrial electron transport and oxidative phosphorylation genes. *Virus Genes* **39**:p 102-112.
86. **Reddy SM, Lupiani B, Gimeno IM, Silva RF, Lee LF, Witter RL.** 2002. Rescue of a pathogenic Marek's disease virus with overlapping cosmid DNAs: Use of a pp38 mutant to validate the technology for the study of gene function. *Proceedings of the National Academy of Sciences* **99**:p 7054-7059.
87. **Rich PR.** 2003. The molecular machinery of Keilin's respiratory chain. *Biochemical Society Transactions* **31**:p 1095-1105.
88. **Rispens B, van Vloten H, Mastenbroek N, Maas H, Schat K.** 1972. Control of Marek's disease in the Netherlands. I. Isolation of an avirulent Marek's disease virus (strain CVI 988) and its use in laboratory vaccination trials. *Avian Diseases* **16**:p 108-125.
89. **Rispens B, van Vloten H, Mastenbroek N, Maas H, Schat K.** 1972. Control of Marek's disease in the Netherlands. II. Field trials on vaccination with an avirulent strain (CVI 988) of Marek's disease virus. *Avian Diseases* **16**:p 126-138.

90. **Robey IF, Lien AD, Welsh SJ, Baggett BK, Gillies RJ.** 2005. Hypoxia-inducible factor-1a and the glycolytic phenotype in tumors. *Neoplasia* **7**:p 324-330.
91. **Rong Y, Wu W, Ni X, Kuang T, Jin D, Wang D, Lou W.** 2013. Lactate dehydrogenase A is overexpressed in pancreatic cancer and promotes the growth of pancreatic cancer cells. *Tumor Biol.*p 1-8.
92. **Sarma G, Greer W, Gildersleeve RP, Murray D, Miles A.** 1995. Field safety and efficacy of in ovo administration of HVT + SB-1 bivalent Marek's disease vaccine in commercial broilers. *Avian Diseases* **39**:p 211-217.
93. **Schat KA, Calnek BW.** 1978. Characterization of an apparently nononcogenic Marek's disease virus. *Journal of the National Cancer Institute* **107**:p 1075-1082.
94. **Semenza GL.** 2011. Regulation of metabolism by hypoxia-inducible factor 1. *Cold Spring Harbor Symposia on Quantitative Biology* **76**:p 347-353.
95. **Semenza GL.** 2007. Oxygen-dependent regulation of mitochondrial respiration by hypoxia-inducible factor 1. *Biochemical Journal* **405**:p 1-9.
96. **Semenza GL.** 2008. Tumor metabolism: cancer cells give and take lactate. *J Clin Invest* **118**:p 3835-3837.
97. **Semenza GL.** 2010. HIF-1: upstream and downstream of cancer metabolism. *Current Opinion in Genetics & Development* **20**:p 51-56. doi:doi: 10.1016/j.gde.2009.10.009.
98. **Shack LA, Buza JJ, Burgess SC.** 2008. The neoplastically transformed (CD30hi) Marek's disease lymphoma cell phenotype most closely resembles T-regulatory cells. *Cancer Immunol Immunother* **57**:p 1253-1262.
99. **Shamblin CE, Greene N, Arumugaswami V, Dienglewicz RL, Parcells MS.** 2004. Comparative analysis of Marek's disease virus (MDV) glycoprotein-, lytic antigen pp38- and transformation antigen Meq-encoding genes: association of meq mutations with MDVs of high virulence. *Veterinary Microbiology* **102**:p 147-167.
100. **Shkreli M, Dambrine G, Soubieux D, Kut E, Rasschaert D.** 2007. Involvement of the oncoprotein c-Myc in viral telomerase RNA gene regulation during Marek's disease virus-induced lymphomagenesis. *Journal of Virology* **81**:p 4848-4857.

101. **Spatz SJ, Petherbridge L, Zhao Y, Nair V.** 2007. Comparative full-length sequence analysis of oncogenic and vaccine (Rispens) strains of Marek's disease virus. *Journal of General Virology* **88**:p 1080-1096.
102. **Spatz S, Schat K.** 2011. Comparative genomic sequence analysis of the Marek's disease vaccine strain SB-1. *Virus Genes* **42**:p 331-338.
103. **Suzuki S, Tanaka T, Poyurovsky MV, Nagano H, Mayama T, Ohkubo S, Lokshin M, Hosokawa H, Nakayama T, Suzuki Y, Sugano S, Sato E, Nagao T, Yokote K, Tatsuno I, Prives C.** 2010. Phosphate-activated glutaminase (GLS2), a p53-inducible regulator of glutamine metabolism and reactive oxygen species. *Proceedings of the National Academy of Sciences* **107**:p 7461-7466.
104. **Tannock IF, Rotin D.** 1989. Acid pH in tumors and its potential for therapeutic exploitation. *Cancer Research* **49**:p 4373-4384.
105. **Trimpin S, Brizzard B.** 2009. Analysis of insoluble proteins. *BioTechniques* **46**:p 321-326.
106. **Tristan C, Shahani N, Sedlak TW, Sawa A.** 2011. The diverse functions of GAPDH: Views from different subcellular compartments. *Cellular Signalling* **23**:p 317-323.
107. **Tulman ER, Afonso CL, Lu Z, Zsak L, Rock DL, Kutish GF.** 2000. The genome of a very virulent Marek's disease virus. *Journal of Virology* **74**:p 7980-7988.
108. **Turowski GA, Rashid Z, Hong F, Madri JA, Basson MD.** 1994. Glutamine modulates phenotype and stimulates proliferation in human colon cancer cell lines. *Cancer Research* **54**:p 5974-5980.
109. **Ullah MS, Davies AJ, Halestrap AP.** 2006. The plasma membrane lactate transporter MCT4, but not MCT1, is up-regulated by hypoxia through a HIF-1a dependent mechanism. *Journal of Biological Chemistry* **281**:p 9030-9037.
110. **Vander Heiden MG, Cantley LC, Thompson CB.** 2009. Understanding the Warburg effect: The metabolic requirements of cell proliferation. *Science* **324**:p 1029-1033.

111. **Vandesompele J, De Preter K, Pattyn F, Poppe B, Van Roy N, De Paepe A, Speleman F.** 2002. Accurate normalization of real-time quantitative RT-PCR data by geometric averaging of multiple internal control genes. *Genome Biology* **3**:p research0034. doi:10.1186/gb-2002-3-7-research0034.
112. **Vogel C, Marcotte EM.** 2012. Insights into the regulation of protein abundance from proteomic and transcriptomic analyses. *Nat Rev Genet* **13**:p 227-232.
113. **Wagstaff P, Kang HY, Mylott D, Robbins PJ, White MK.** 1995. Characterization of the avian GLUT1 glucose transporter: differential regulation of GLUT1 and GLUT3 in chicken embryo fibroblasts. *Molecular Biology of the Cell* **6**:p 1575-1589.
114. **Warburg O.** 1956. On the origin of cancer cells. *Science* **123**:p 309-314.
115. **Werth N, Beerlage C, Rosenberger C, Yazdi AS, Edelmann M, Amr A, Bernhardt W, von Eiff C, Becker K, Sch+ñfer A, Peschel A, Kempf VAJ.** 2010. Activation of hypoxia inducible factor 1 is a general phenomenon in infections with human pathogens. *PLoS ONE* **5**:p e11576. doi:doi:10.1371/journal.pone.0011576.
116. **Wise DR, Thompson CB.** 2010. Glutamine addiction: a new therapeutic target in cancer. *Trends in Biochemical Sciences* **35**:p 427-433.
117. **Witter RL.** 1997. Increased virulence of Marek's disease virus field isolates. *Avian Diseases* **149**:p 149-163.
118. **Witter RL.** 1998. The changing landscape of Marek's disease. *Avian Pathology*.
119. **Witter RL, Sharma J, Lee LF, Opitz H, Henry C.** 1984. Field trials to test the efficacy of polyvalent Marek's disease vaccines in broilers. *Avian Diseases* **28**:p 44-60.
120. **Witter RL, Schat KA, Saif YM.** 2003. Marek's Disease, p 407-465. *In: Diseases of Poultry*.
121. **Xiao L, Hu Z, Dong X, Tan Z, Li W, Tang M, Chen L, Yang L, Tao Y, Jiang Y, Li J, Yi B, Li B, Fan S, You S, Deng X, Hu F, Feng L, Bode AM, Dong Z, Sun L, Cao Y.** 2014. Targeting Epstein-Barr virus oncoprotein LMP1-mediated glycolysis sensitizes nasopharyngeal carcinoma to radiation therapy. *Oncogene*. doi:Original Article.

122. **Xie Q, Anderson AS, Morgan RW.** 1996. Marek's disease virus (MDV) ICP4, pp38, and meq genes are involved in the maintenance of transformation of MDCC-MSB-1 MDV-transformed lymphoblastoid cells. *Journal of Virology* **70**:p 1125-1131.
123. **Yao F, Zhao T, Zhong C, Zhu J, Zhao H.** 2013. LDHA is necessary for the tumorigenicity of esophageal squamous cell carcinoma. *Tumor Biol.* **34**:p 25-31.
124. **Yeung S, Pan J, Lee MH.** 2008. Roles of p53, Myc and HIF-1 in regulating glycolysis and the seventh hallmark of cancer. *Cellular and Molecular Life Sciences* **65**:p 3981-3999. doi:10.1007/s00018-008-8224-x.
125. **Yin R, Liu X, Liu C, Ding Z, Zhang X, Tian F, Liu W, Yu J, Li L, Hrab de Angelis M, Stoeger T.** 2011. Systematic selection of housekeeping genes for gene expression normalization in chicken embryo fibroblasts infected with Newcastle disease virus. *Biochemical and Biophysical Research Communications* **413**:p 537-540. doi:doi: 10.1016/j.bbrc.2011.08.131.
126. **You L, Yin J.** 2000. Patterns of regulation from mRNA and protein time series. *Metabolic Engineering* **2**:p 210-217.
127. **Yu Y, Maguire TG, Alwine JC.** 2011. Human cytomegalovirus activates glucose transporter 4 expression to increase glucose uptake during infection. *Journal of Virology* **85**:p 1573-1580.
128. **Yuan J, Cahir-McFarland E, Zhao B, Kieff E.** 2006. Virus and cell RNAs expressed during Epstein-Barr Virus replication. *Journal of Virology* **80**:p 2548-2565.
129. **Zhao B, Maruo S, Cooper A, Chase R, Johannsen E, Kieff E, Cahir-McFarland E.** 2006. RNAs induced by Epstein-Barr virus nuclear antigen 2 in lymphoblastoid cell lines. *Proceedings of the National Academy of Sciences of the United States of America* **103**:p 1900-1905.
130. **Zhao Y, Butler E, Tan M.** 2013. Targeting cellular metabolism to improve cancer therapeutics. *Cell Death and Disease* **4**:p e532.

## Appendix A

### WESTERN BLOT ANALYSIS RESULTS

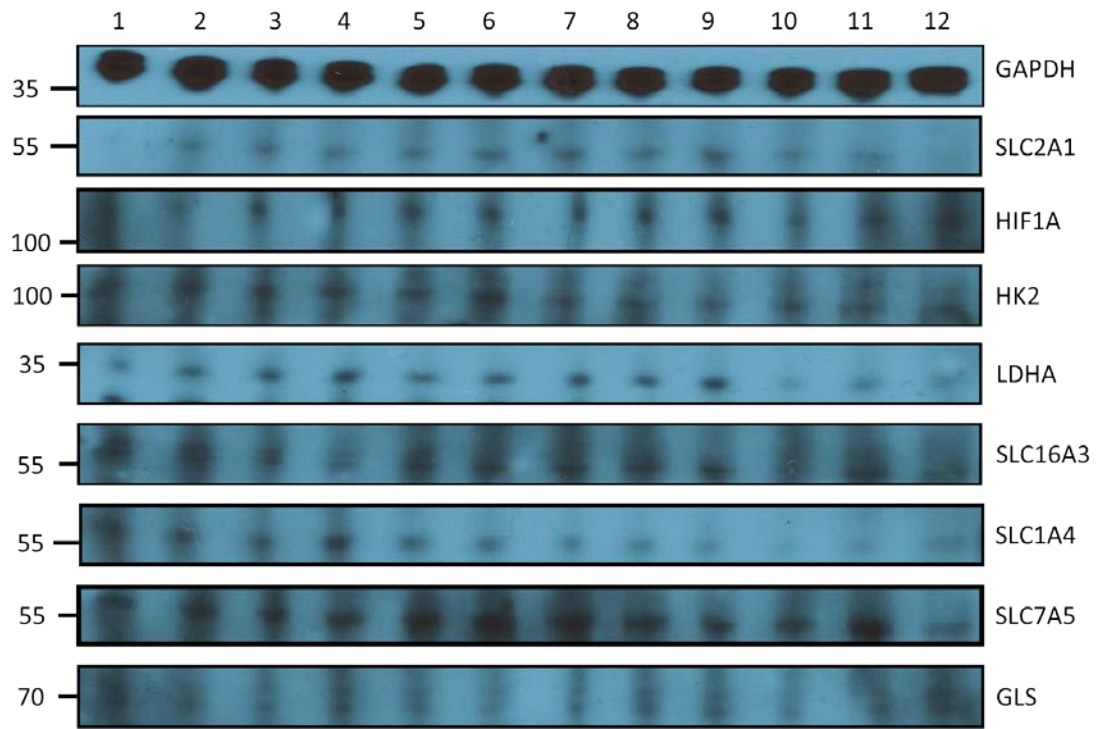


**Figure A1** Western blot analysis of mock infected CEF (wells 1-3) and CEF infected with CU2 (wells 4-6), RB-1B (wells 7-9), and TKING MDV strains (wells 10-12).

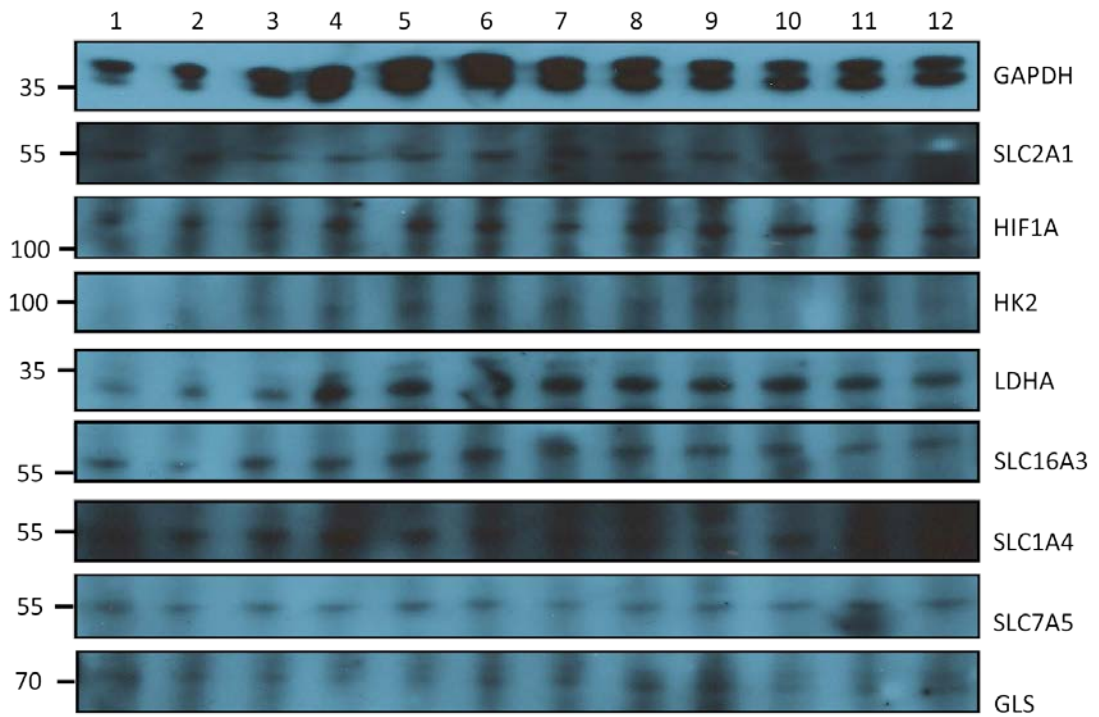


**Figure A2** Western blot analysis of mock infected CEFs (wells 1-3) and CEFs infected with HVT (wells 4-6), SB-1 (wells 7-9), and CVI-988 MDV strains (wells 10-12).

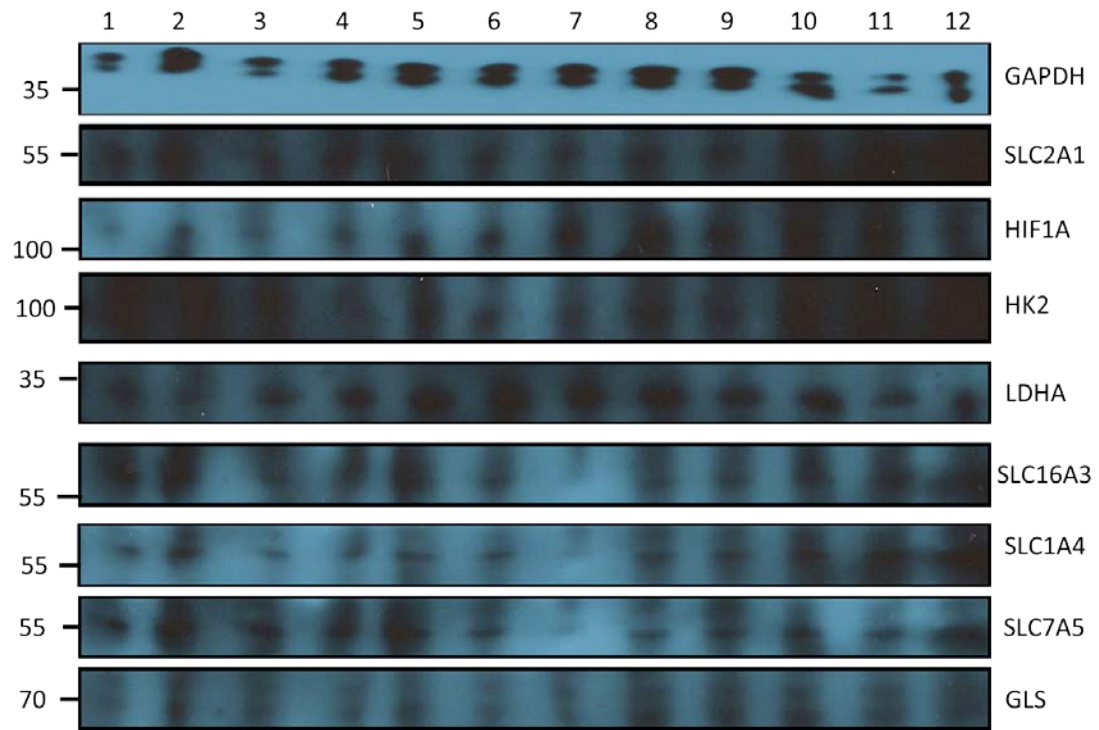


**Figure A3** Western blot analysis of mock infected CEFs (wells 1-3) and CEFs infected with Md5 (wells 4-6), Md5Δmeq (wells 7-9), and Md5Δpp38 MDV strains (wells 10-12).

## **Appendix B**

### **PERMISSION LETTER**

The animal use in this study was approved under the Ag Animal Care and Use Committee (AACUC) blanket Vaccine Trial protocol: (22) 04-15-10a. Further, this trial was filed under the one-page form marked by the date: 01-07-12.